Interconversion of Planar and Nonplanar *N*-Amido Ligands. Thermodynamically Stable Nonplanar *N*-Amido Ligands

Fred C. Anson, Terrence J. Collins,*[1] Stephen L. Gipson, John T. Keech, Terry E. Krafft, and Geoffrey T. Peake

Contribution No. 7341 from The Chemical Laboratories, California Institute of Technology, Pasadena, California 91125. *Received March 10, 1986*

Abstract: An unexpected structural feature of organic amido ligating, polyanionic chelating (PAC) ligands has been discovered. Oxidation of *trans*-Os(η^4-**1**)(*t*-Bupy)$_2$, **3** (H_4**1** = 1,2-bis(3,5-dichloro-2-hydroxybenzamido)-4,5-dichlorobenzene), by 1 faraday per mol yields an equilibrium mixture of $\mathbf{3}^+$ and the cis-α diastereomer, $\mathbf{4}^+$. Subsequent one-electron reduction with ferrocene produces a separable nonequilibrium mixture of **3** and **4**. Compound **4** contains nonplanar N-coordinated organic amido ligands, whereas **3** contains planar *N*-amido ligands. The equilibrium constant at 22 °C for the process $\mathbf{3}^+ \rightleftharpoons \mathbf{4}^+$ has been measured

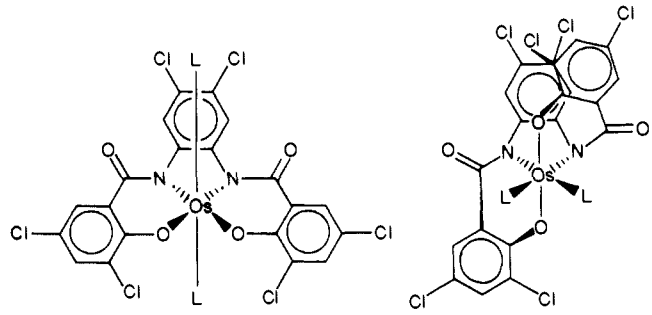

3 **4**

by normal pulse voltammetry and used with the formal potentials for the three successive reductions of $\mathbf{3}^+$ and $\mathbf{4}^+$ to calculate the trans $\rightleftharpoons$ cis-α equilibrium constants at the osmium(IV), -(III), and -(II) oxidation states, K^0, K^-, and K^{2-}, respectively. The cis-α ligand complement becomes increasingly favored as the oxidation state is increased, suggesting that it is more donating than the trans complement. The K^0 equilibrium constants for the series, *cis*-α-Os(η^4-**1**)(*p*-X-py)$_2$ $\rightleftharpoons$ *trans*-Os(η^4-**1**)(*p*-X-py)$_2$ [X = MeO, *t*-Bu, Et, Me, H, Cl, Br, and CH_3CO], were correlated with the Fischer $\bar{\sigma}$ substituent constants for pyridinium ion dissociations (ρ = 2.1, r = 0.95) and with the σ_p substituent constants (ρ = −1.6, r = 0.95). The relationships suggest that the equilibria respond to electronic effects. As the ancillary pyridine ligands become less donating, the equilibrium favors the more donating cis-α complement. At the osmium(IV) stage the trans diastereomer is thermodynamically stable for the bispyridine complexes. Coordination of an electron-withdrawing π-acid ligand causes the cis-α diastereomer to become thermodynamically favored at the osmium(IV) state, reinforcing the theme that electron deficient metal centers favor the more donating cis-α ligand complement. When the two monodentate ligands are large, as for *trans*-Os(η^4-**1**)(PPh_3)$_2$, the trans isomer is observed at all oxidation states, suggesting that steric effects can also play a role. The formal potential data correlate well with $\bar{\sigma}$. When the formal potential data are converted to equilibrium constants, the ρ values vary from 2.39 to 9.17. *p*-Acetylpyridine exhibits normal behavior in the monocation/osmium(IV) couples, but deviations are found for the (IV/III) and (III/II) couples which become more marked as the couples become more negative. The deviations suggest that *p*-acetylpyridine has a greater electron-withdrawing capacity when coordinated to osmium(III) or osmium(II) than expected from the correlations with the other pyridines. The CV data reveal that the cis-α complexes are markedly weaker oxidants than the trans analogues. The formal potentials are reduced by up to 510 mV. Evidence is presented which suggests that the nonplanar *N*-amido ligands in the cis-α complexes are the principal sources of this reduction in oxidizing power and of the related increased donor capacity of the cis-α ligand complements.

The search for new inorganic oxidizing agents is an emerging interdisciplinary pursuit.[2] We are developing new highly oxidized and highly oxidizing inorganic complexes by utilizing polyanionic chelating (PAC) ligands that contain oxidation resistant donors, including N-coordinated organic amido groups (e.g., **1** and **2**[3]).[4-8]

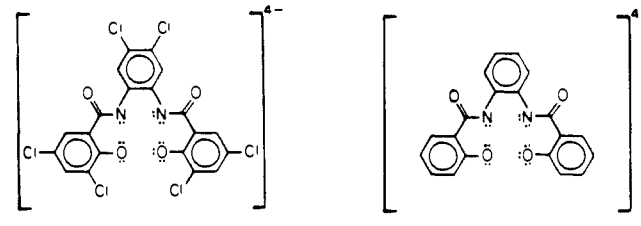

1 **2**

The oxidizing properties of an inorganic complex are determined to a significant extent by the donor properties of the ligand complement. An understanding of these properties is a major factor in the design of inorganic redox systems. While it is well-known that planar N-coordinated organic amido (or amidyl)

(1) Alfred P. Sloan Research Fellow, 1986–1988; Dreyfus Teacher-Scholar 1985–1989.

(2) (a) Report of the International Workshop on *Activation of Dioxygen Species and Homogeneous Catalytic Oxidations*, Collins, T. J., Ed., University of Padua: Galzignano (Padua), Italy, June 28–29, 1984, and references therein. (b) "*Opportunities in Chemistry*"; report of the Committee to Survey Opportunities in the Chemical Sciences; Pimentel, G. C., Chairman; National Academy Press: Washington, 1985, pp 83–84.

(3) Ligand names: 1,2-bis(3,5-dichloro-2-hydroxybenzamido)-4,5-dichlorobenzene, H_4-CHBA-DCB (**1**); 1,2-bis(2-hydroxybenzamido)benzene, H_4-HBA-B (**2**).

(4) (a) Anson, F. C.; Christie, J. A.; Collins, T. J.; Coots, R. J.; Furutani, T. T.; Gipson, S. L.; Keech, J. T.; Krafft, T. E.; Santarsiero, B. D.; Spies, G. H. *J. Am. Chem. Soc.* **1984**, *106*, 4460–4472. (b) Anson, F. C.; Collins, T. J.; Coots, R. J.; Gipson, S. L.; Keech, J. T.; Krafft, T. E.; Santarsiero, B. D.; Spies, G. H., submitted for publication in Inorg. Chem.

(5) Christie, J. A.; Collins, T. J.; Krafft, T. E.; Santarsiero, B. D.; Spies, G. H. *J. Chem. Soc., Chem. Commun.* **1984**, 198–199.

(6) Collins, T. J.; Santarsiero, B. D.; Spies, G. H. *J. Chem. Soc., Chem. Commun.* **1983**, 681–682.

(7) Anson, F. C.; Collins, T. J.; Coots, R. J.; Gipson, S. L.; Richmond, T. G. *J. Am. Chem. Soc.* **1984**, *106*, 5037–5038.

(8) Collins, T. J.; Richmond, T. G.; Santarsiero, B. D.; Treco, B. G. R. T. *J. Am. Chem. Soc.*, in press.

0002-7863/86/1508-6593$01.50/0

ligands are strong donors to transition-metal centers,[4,7-9] the relative donor properties of the nonplanar analogues have not been assessed because of the absence of candidate complexes. Nonplanar amides are rarely encountered.[10,14] We have discovered that *N*-amido containing PAC ligand complexes can isomerize under certain conditions to convert planar *N*-amido ligands to nonplanar forms. Here we present evidence which suggests that nonplanar *N*-amido ligands are even better donors than planar *N*-amido ligands and that the observed planar → nonplanar *N*-amido isomerizations occur so that electron-deficient metal centers can be stabilized by the increased donor capacity.

Experimental Section

Materials. Acetone (Mallinckrodt), acetonitrile (Mallinckrodt), benzene (thiophene free, Aldrich), chloroform (Baker), di-*n*-butyl ether (EM Science), diethyl ether (Baker), ethanol (U.S.I.), hexanes (Aldrich), methanol (Baker), and toluene (Baker) were reagent grade and were used as received, unless otherwise noted. Dichloromethane (Baker) and tetrahydrofuran (Baker) were distilled from calcium hydride prior to use. 1,2-Dichloroethane was distilled from P_2O_5 prior to use. *p*-Acetylpyridine (98%, Aldrich), 2-acetylsalicylic acid (Aldrich), bromoethane (98%, Aldrich), *tert*-butyl isocyanide (Alfa), *p*-*tert*-butylpyridine (99%, Aldrich), carbon monoxide (Matheson), chlorobenzene (99%, Aldrich), 2,2′-dipyridyl (99%, Aldrich), ethylenebis(diphenylphosphine) (97%, Aldrich), *p*-ethylpyridine (98%, Aldrich), hydrochloric acid (concentrated, Mallinckrodt), *o*-iodosylbenzoic acid (Sigma), osmium tetraoxide (99.8%, Alfa), nitrosonium hexafluorophosphate (Pfaltz and Bauer), *p*-picoline (M.C.B.), potassium carbonate (Baker), potassium hydroxide (Baker), sodium hydroxide (Baker), triethylamine (reagent, M.C.B.), trifluoroacetic acid (98.5%, M.C.B.), and triphenylphosphine (99%, Aldrich) were all used as received. Oxalyl chloride (Aldrich) was freshly distilled under nitrogen. The *o*-phenylenediamine (Aldrich) was recrystallized from toluene. A 9.2 M solution of *p*-chloropyridine in diethylether was prepared from *p*-chloropyridine hydrochloride (97%, Lancaster Synthesis) by dissolving it in aqueous 1 M KOH and extracting it into diethylether. Molarity was estimated by ^{1}H NMR spectroscopy. An 8.8 M solution of *p*-bromopyridine in diethylether was prepared similarly from *p*-bromopyridine hydrochloride (95%, Aldrich). *p*-Methoxypyridine was prepared from its N-oxide (Lancaster Synthesis) by using PCl_3 by the method of Ochiai.[11] Silica gel used in column chromatography was 60-200 mesh (Davison). Preparatory TLC plates were silica gel (GF2000, Analtech).

Physical Measurements. ^{1}H NMR spectra were recorded at 90 MHz on a Varian EM-390 spectrometer, at 89.83 MHz on a JEOL FX90-Q spectrometer, at 399.7822 MHz on a JEOL GX-400 spectrometer, or at 500.135 MHz on a Bruker WM-500 spectrometer. ^{1}H chemical shifts are reported in ppm (δ) vs. Me_4Si with the solvent ($CDCl_3$ δ 7.24, CD_2Cl_2 δ 5.32, Me_2SO-d_6 δ 2.49, or Me_2CO-d_6 δ 2.04) as internal standard. ^{31}P NMR spectra were recorded at 36.28 MHz on a JEOL FX-90Q spectrometer or at 109.352 MHz on an IBM/Bruker WP-270SY spectrometer. ^{31}P chemical shifts are reported in ppm (δ) vs. 85% H_3PO_4 as external standard. Infrared spectra were recorded on a Beckman IR 4240 spectrophotometer or on a Mattson Serius 100 FTIR spectrophotometer. Elemental analyses were obtained at the Caltech analytical facility. Solvents of crystallization were quantified by ^{1}H NMR spectroscopy of the authentic samples submitted for elemental analyses.

Magnetic Susceptibility Measurements. Magnetic susceptibility measurements were performed on an S.H.E. 905 SQUID susceptometer at the University of Southern California. Measurements were recorded between 6 and 300 K on typical sample sizes of 20–80 mg. The following diamagnetic corrections were applied, χ_0 (cgs/mol): **1**, -168×10^{-6}; **2**, -20×10^{-6}; PPh_3, -167×10^{-6}; $OPPh_3$, -168×10^{-6}; dppe, -85×10^{-6}; py, -49×10^{-6}; bipy, -192×10^{-1}. All paramagnatic osmium(IV) compounds exhibited temperature independent paramagnetism, TIP, with negligible Curie–Weiss behavior. The χ_m values for *trans*-Os(η^4-**1**)-$(PPh_3)_2$ increased at low temperature (6–50 K) suggesting that small amounts of paramagnetic impurities were present. The following χ_m values are the averaged data between 100 and 300 K (cgs/mol): *trans*-Os(η^4-**1**)$(PPh_3)_2$, 952×10^{-6}; *trans*-Os(η^4-**2**)$(PPh_3)_2$, 788×10^{-6}; *cis*-β-Os(η^4-**1**)(dppe), 303×10^{-6}; *trans*-Os(η^4-**1**)$(OPPh_3)_2$, 1030×10^{-6}; *trans*-Os(η^4-**1**)$(py)_2$, 1400×10^{-6}; *cis*-β-Os(η^4-**1**)(bipy), 877×10^{-6}.

Electrochemical Procedures. Dichloromethane (Mallinckrodt) used in cyclic voltammetric experiments was reagent grade and was further purified by passing it through a short column of activated alumina (Woelm N. Akt. I). For controlled-potential electrolysis experiments, the dichloromethane was dried over calcium hydride and vacuum transferred into the cell. TBAP supporting electrolyte (Southwestern Analytical Chemicals) was dried, recrystallized twice from acetone/ether, and then dried in vacuo. The TBAP concentration in all solutions was 0.1 M. The Pt disc electrode (0.03 cm^2), used for cyclic voltammetry, was polished with 0.3 micron alumina polishing powder (Linde), sonicated, and then rinsed with water, acetone, and methylene chloride. BPG electrodes (Union Carbide Co., Chicago) used for cyclic voltammetry were cut and mounted as previously described.[12b] The reference electrode was either a saturated KCl silver–silver chloride electrode (Ag/AgCl) or a silver wire quasireference electrode. In all cases ferrocene was added at the conclusion of the experiment as an internal potential standard. All potentials are quoted with respect to the formal potential of the ferrocinium/ferrocene couple which, under these conditions, we have consistently measured in dichloromethane as +0.48 V vs. SCE or ca. +0.70 V vs. NHE and in acetonitrile as +0.39 V vs. SCE.

Cyclic voltammetry and controlled-potential electrolyses were performed with a Princeton Applied Research Model 173/179 potentiostat/digital coulometer equipped with positive feedback IR-compensation and a Model 175 universal programmer. Current-voltage curves were recorded on a Houston Instruments Model 2000 X-Y recorder. Controlled potential electrolysis experiments were conducted in a three-compartment vacuum line electrochemical cell as described elsewhere. Other cyclic voltammetric experiments were conducted in standard two-compartment cells. Working and counter electrodes for controlled-potential electrolysis were Pt-gauze.

Normal pulse voltammetry was used to measure K^+ for the isomerization of $[Os(\eta^4\text{-CHBA-DCB})(p\text{-X-py})_2]^+$ compounds. It was performed on a Bioanalytical Systems, Inc. BAS-100 Electrochemical analyzer. The parameters used were a pulse width of 17 ms and a scan rate of 20 mV/s. Changing the parameters to a pulse period of 5000 ms and a scan rate of 4 mV/s had no effect on the measured equilibrium constant, which

(9) See, for example: (a) Margerum, D. W. *Pure Appl. Chem.* **1983**, *55*, 23–34. (b) Margerum, D. W. *Oxidases Relat. Redox Syst., Proc. Int. Symp., 3rd* **1979**, 193–206. (c) Diaddario, L. L.; Robinson, W. R.; Margerum, D. W. *Inorg. Chem.* **1983**, *22*, 1021–5. (d) Sigel, H.; Martin, R. B. *Chem. Rev.* **1982**, *82*, 385. (e) Kimura, E.; Sakonaka, A.; Machila, R.; Kodama, M. *J. Am. Chem. Soc.* **1982**, *104*, 4255. (f) Buttafava, A.; Fabbrizzi, L.; Perotti, A.; Seghi, B. *J. Chem. Soc., Chem. Commun.* **1982**, 1166–7. (g) Fabbrizzi, L.; Perotti, A.; Poggi, A. *Inorg. Chem.* **1983**, *22*, 1411–12. (h) Buttafava, A.; Fabbrizzi, L.; Perotti, A.; Poggi, A.; Seghi, B. *Inorg. Chem.* **1984**, *23*, 3917–22.

(10) Nonplanar amides are found for formamide,[a] for some constrained molecules such as certain lactams[b-w] and anti-Bredt bridgehead nitrogen compounds,[x-z5] and for some complexes of PAC ligands.[14] (a) Costain, C. C.; Dowling, J. M. *J. Chem. Phys.* **1960**, *32*, 158–165. (b) Winkler, F. K.; Dunitz, J. D. *Acta Crystallogr., Sect. B: Struct. Crystallogr. Cryst. Chem.* **1975**, *B31*, 270–272. (c) Winkler, F. K.; Dunitz, J. D. *Ibid.* **1975**, *B31*, 276–278. (d) Winkler, F. K.; Dunitz, J. D. *Ibid.* **1975**, *B31*, 281–283. (e) Winkler, F. K.; Dunitz, J. D. *Ibid.* **1975**, *B31*, 283–286. (f) Smolíková, J.; Tichý, M.; Bláha, K. *Collect. Czech. Chem. Commun.* **1978**, *41*, 413–429. (g) Kálal, P.; Bláha, K.; Langer, V. *Acta Crystallogr., Sect. C: Cryst. Struct. Commun.* **1984**, *C40*, 1242–1245. (h) Hossain, M. B.; Baker, J. R.; van der Helm, D. *Acta Crystallogr., Sect. B: Struct. Crystallogr. Cryst. Chem.* **1981**, *B37*, 575–579. (i) Barnes, C. L.; McGuffey, F. A.; van der Helm, D. *Acta Crystallogr., Sect. C: Cryst. Struct. Commun.* **1985**, *C41*, 92–95. (j) Paquette, L. A.; Kakihana, T.; Hansen, J. F.; Philips, J. C. *J. Am. Chem. Soc.* **1971**, *93*, 152–161. (k) Blackburn, G. M.; Plackett, J. D. *J. Chem. Soc., Perkin Trans. 2* **1972**, 1366–1371. (l) Dunitz, J. D.; Winkler, F. K. *J. Mol. Biol.* **1971**, *59*, 169–182. (m) Dunitz, J. D.; Winkler, F. K. *Acta. Crystallogr., Sect. B: Struct. Crystallogr. Cryst. Chem.* **1975**, *B31*, 251–263. (n) Sweet, R. M.; Dahl, L. F. *J. Am. Chem. Soc.* **1970**, *92*, 5489. (o) Woodward, R. B. *Recent Advances in the Chemistry of β-Lactam Antibiotics*; Elks, J., Ed.; Chemical Society: London, 1977; pp 167–180. (p) Butler, A. R.; Freeman, K. A.; Wright, D. E. *Ibid.* Elks, J., Ed.; pp 299–303. (q) Proctor, P.; Gensmantel, N. P.; Page, M. I. *J. Chem. Soc., Perkin Trans. 2* **1982**, 1185–1192. (r) Page, M. I. *Acc. Chem. Res.* **1984**, *17*, 144–151. (s) Smolíková, J.; Koblicová, Z.; Bláha, K. *Collect. Czech. Chem. Commun.* **1973**, *38*, 532–547. (t) Bláha, K.; Buděšinshý, M.; Doblicová, Z.; Maloň, P.; Tichý, M.; Baker, J.; Hossain, M.; van der Helm, D. *Ibid.* **1982**, *47*, 1000–1019. (u) Ealick, S. E.; van der Helm, D. *Acta Crystallogr., Sect B: Struct. Crystallogr. Cryst. Chem.* **1975**, *B31*, 2676–2680. (v) Ealick, S. E.; Washecheck, D. M.; van der Helm, D. *Ibid.* **1976**, *B32*, 895–900. (w) Ealick, S. E.; van der Helm, D. *Ibid.* **1977**, *B33*, 76–80. (x) Pracejus, H. *Chem. Ber.* **1959**, *92*, 988–998. (y) Pracejus, H. *Ibid.* **1965**, *98*, 2897–2905. (z) Pracejus, H.; Kehlen, M.; Khlen, H.; Matschiner, H. *Tetrahedron* **1965**, *21*, 2257–2270. (z1) Hall, H. K., Jr.; Shaw, R. G., Jr.; Deutschmann, A. *J. Org. Chem.* **1980**, *45*, 3722–3724. (z2) Hall, H. K., Jr.; El-Shekeil, A. *Ibid.* **1980**, *45*, 5325–5328. (z3) Hall, H. K., Jr.; El-Shekeil, A. *Chem. Rev.* **1983**, *83*, 549–555. (z4) Buchanan, G. L. *J. Chem. Soc., Perkin Trans. 1* **1984**, 2669–2670. (z5) Coqueret, X.; Bourelle-Wargnier, F.; Chuche, J. *J. Org. Chem.* **1985**, *50*, 910–912.

(11) Ochiai, E. *Aromatic Amine Oxides*; Mizoguchi, D. O., Translator, Elsevier: New York, 1967; p 195.

(12) (a) Peters, D. G.; Hayes, J. M. *Chemical Separations and Measurements; Theory and Practice of Analytical Chemistry*; W. B. Saunders: Philadelphia, 1974; pp 6–37. (b) Oyama, N.; Anson, F. C. *J. Am. Chem. Soc.* **1979**, *101*, 3450–3456.

was taken to be equal to the ratio of wave heights of the two Os(IV/III) reductions. Standard two- and three-compartment electrochemical cells were used.

Derivation of Successive Equilibrium Constants

Given the following scheme

$$\begin{array}{ccc} 4^+ + Fc & \rightleftharpoons & 3^+ + Fc \\ E_c^f \downarrow\uparrow & & \downarrow\uparrow E_t^f \\ 4 + Fc^+ & \rightleftharpoons & 3 + Fc^+ \end{array}$$

where K^+ is determined by normal pulse voltammetry and E_t^f and E_c^f are determined by cyclic voltammetry; K^0 can be calculated as follows. Since

$$\Delta G^+ = -RT\ln K^+ = G(3^+) - G(4^+)$$

and

$$\Delta G(3^+/3) = -FE_t^f = G(3) + G(Fc^+) - G(3^+) - G(Fc)$$

$$\Delta G(4^+/4) = -FE_c^f = G(4) + G(Fc^+) - G(4^+) - G(Fc)$$

then

$$\Delta G^+ + \Delta G(3^+/3) - \Delta G(4^+/4) = G(3) - G(4) = \Delta G^\circ$$

Alternatively

$$K^0 = K^+ \exp\left[\frac{F}{RT}(E_t^f - E_c^f)\right]$$

which at 22 °C can be expressed in the general form

$$K^n = K^{n+1} \exp[39.32(E_t^{f(n+1/n)} - E_c^{f(n+1/n)})]$$

Errors were propagated according to the equation

$$\sigma_F^2 = \left[\sum_i \left(\frac{\delta F}{\delta x_i}\right)^2 \sigma^2_{x_i}\right]^{1/2}$$

where $F = F(x_1, x_2, \ldots, x_n)$. Uncertainties were calculated at the 95% confidence level.[12a] Errors of ±5 mV for E^f and ±2 K for temperature were assumed.

Syntheses. All reactions were carried out in air unless otherwise noted. $K_2[Os(OH)_4(O)_2]$,[13] 3,5-dichloroacetylsalicyclic acid, H_4CHBA-DCB, K_2[*trans*-Os(η^4-CHBA-DCB)$(O)_2$],[4] *trans*-Os-(η^4-CHBA-DCB)$(PPh_3)_2$,[4] *trans*-Os-(η^4-CHBA-DCB)(*t*-Bupy)$_2$,[4] *cis*-α-Os(η^4-CHBA-DCB)(*t*-BuNC)$_2$,[4] *cis*-α-Os(η^4-CHBA-DCB)(PPh_3)(*t*-BuNC),[14] and *cis*-α-Os(η^4-HBA-B)$(CO)(PPh_3)$[14] were prepared as described in the literature.

H_4HBA-B (2). 2-Acetylsalicyclic acid (50.0 g, 0.27 mol) was heated at 30 °C in oxalyl chloride under a nitrogen atmosphere (4 h). Excess oxalyl chloride was removed under reduced pressure. The residue was dissolved in dichloromethane (30 mL), and the dichloromethane was removed in vacuo. This washing process was repeated 3 times. The residue was then dissolved in dichloromethane (100 mL) and chilled on an ice bath. This solution was added dropwise to a stirred, chilled solution of *o*-phenylenediamine (15.0 g, 0.138 mol) in dichloromethane (100 mL) that was cooled continuously on an ice bath. The mixture was stirred (1 h), excess (>1 equiv) triethylamine was added, and the mixture was again stirred (0.5 h). The mixture was treated with 6 M NaOH solution (100 mL), and the organic volatiles were removed on a rotary evaporator. The remaining aqueous solution was decanted from the undissolved organic residue. The residue was dissolved in a small amount of acetone and then treated with an additional portion of 6 M NaOH solution (100 mL). The aqueous solutions were combined and slowly acidified with concentrated HCl. The precipitate was collected, washed with water, and recrystallized from acetone/water: yield 78.3 g (81%); ^{1}H NMR (Table I); IR (Njuol) 1640 cm^{-1} ν_{CO} (amide), 1610 cm^{-1} ν_{CO} (amide), 1590 cm^{-1} ν_{CO} (amide). Anal. Calcd for $C_{20}H_{16}N_2O_4$: C, 68.96; H, 4.63; N, 8.04. Found: C, 69.04; H, 4.75; N, 8.14.

(13) Malin, J. M. *Inorg. Synth.* **1980**, *20*, 61.
(14) Collins, T. J.; Coots, R. J.; Furutani, T. T.; Keech, J. T.; Peake, G. T.; Santarsiero, B. D. *J. Am. Chem. Soc.*, in press.

Table I. ^{1}H NMR Data for all Compounds of PAC Ligand [η^4-HBA-B]$^{4-}$, **2**[a]

compound	chelate ligand												other					
								H_o	H_m	H_p								
H_4-**2**[b,d]	6.8–7.1	7.2–7.6	7.7–7.8	7.9–8.1	10.1													
	m	m	m	m	br s													
	4 H	4 H	2 H	2 H														
K_2[Os(η^4-**2**)$(O)_2$][b,d]	6.4–6.9	8.3	9.1															
	m	dd	dd															
	8 H	2 H	2 H															
		(8, 2)	(7, 3)															
Os(η^4-**2**)$(PPh_3)_2$[c,e]	−4.33	−3.95	1.33	4.27	6.99	8.19		8.28	6.99	7.36								
	t(dd)	dd	d	dd	*f*	m		d	t	t								
	2 H	2 H	2 H	2 H	2 H	2 H		12 H	12 H	6 H								
	(7)	(6, 3)	(8)	(6, 3)	*f*			(7)	(7)	(7)								
Os(η^4-**2**)(PPh_3)(*t*-BuNC)[c,e]	5.66	6.58	6.81	6.90	7.30	7.51	7.95	8.26		7.2–7.4		9.00					1.30	
	d	m	t	m	*g*	t	d	d		m		d					s	
	1 H	3 H	1 H	2 H	1 H	1 H	1 H	1 H		15 H		1 H					9 H	
											dppe Aromatic					dppe Bridge		
Os(η^4-**2**)(dppe), 13[c,e]	5.32	5.46	5.56	5.59	5.65	5.97	6.22	7.1–7.33	7.35	9.81	6.70	6.80	6.85	7.03	7.1–7.33	7.48	7.93	2.07	2.99	3.42	3.97
	d	t	t	t	d	d	t	m	t	d	t	t	t	t	m	d	t	br d	br s	br s	br s
	1 H	1 H	1 H	1 H	1 H	1 H	1 H	3 H	1 H	1 H	2 H	2 H	2 H	4 H	4 H	4 H	2 H	1 H	1 H	1 H	1 H
	(9)	(7)	(8)	(8)	(9)	(9)	(8)		(7)	(9)	(10)	(7)	(9)	(8)		(7)	(9)				

[a] The chemical shifts of paramagnetic osmium(IV) species are somewhat concentration dependent. Coupling constants given in parentheses. [b] Measured at 90 MHz. [c] Measured at 500 MHz. [d] δ in $(CD_3)_2CO$. [e] δ in $CDCl_3$. [f] Hidden by phosphine H_m signal. [g] Hidden by phosphine signal.

Table II. ^{31}P NMR Data

compound	chem shift[a]
trans-Os(η^1-**1**)$(PPh_3)_2$[b]	-789.0
cis-β-Os(η^4-**1**)(dppe), **13**[c]	-992.9, -1015.6
cis-β-Os(η^4-**2**)(dppe), **14**[b]	-64.1, -86.6
trans-Os(η^4-**1**)$(OPPh_3)_2$, **15**[b]	143.9
cis-α-Os(η^4-**1**)$(OPPh_3)_2$, **16**[b,d]	108.4

[a] δ vs. 85% H_3PO_4 in $CDCl_3$, proton decoupled. (*b*) Measured at 36.28 MHz on a JEOL FX90Q spectrometer. (*c*) Measured at 109.352 MHz on an IBM/Bruker WP-270SY spectrometer. (*d*) Measured at -20 °C.

K_2[*trans*-Os(η^4-HBA-B)$(O)_2$]·H_2O. A solution of $K_2[Os(OH)_4(O)_2]$ (2.01 g, 5.46 mmol) in methanol (500 mL) was added to a solution of H_4HBA-B (1.90 g, 5.46 mmol) in THF (200 mL) that was continuously stirred. Excess anhydrous potassium carbonate (2 g) was added, and the mixture was stirred while being heated (ca. 40 °C; 0.5 h). After cooling, the mixture was filtered to remove the K_2CO_3, and the clear brown solution was evaporated to dryness on a rotary evaporator. The residue was dissolved in ethanol, di-*n*-butyl ether was added, and the ethanol was removed on a rotary evaporator to give brown crystals. The product was filtered and washed with diethyl ether: yield 3.60 g (100%); ^1H NMR (Table I); IR (Nujol) 1600 cm^{-1} ν_{CO}(planar amide). Anal. Calcd for $C_{20}H_{12}N_2K_2O_4Os·H_2O$: C, 36.25; H, 2.13; N, 4.23. Found: C, 36.35; H, 2.40; N, 4.07.

***trans*-Os(η^4-HBA-B)$(PPh_3)_2$.** K_2[*trans*-Os(η^4-HBA-B)$(O)_2$]·H_2O (1.02 g, 1.58 mmol) and triphenylphosphine (2.0 g, 6.32 mmol) were dissolved in a mixture of ethanol (25 mL) and THF (45 mL). Excess CF_3CO_2H (0.5 mL) was added, and the solution was stirred at room temperature (10 min), during which time the solution turned from brown to a dark green. Ethanol (20 mL) was added, and the THF was removed on a rotary evaporator to give dark green crystals. The product was filtered and washed with ethanol and hexanes. The solid was recrystallized from CH_2Cl_2/ethanol containing PPh_3 (250 mg). The final product was filtered and washed with ethanol and hexanes: yield 1.23 g (73%); ^1H NMR (Table I); IR (Nujol) 1605 cm^{-1} ν_{CO}(planar amide). Anal. Calcd for $C_{56}H_{42}N_2O_4OsP_2·0.5(H_2O)·0.5(CH_3CH_2OH)$: C, 62.74; H, 4.26; N, 2.57. Found: C, 62.67; H, 4.44; N, 2.45.

***cis*-α-Os(η^4-HBA-B)(PPh_3)(*t*-BuNC).** Benzene (100 mL) was degassed with a nitrogen stream (20 min), *trans*-Os(η^4-HBA-B)$(PPh_3)_2$ (500 mg, 0.472 mmol) was added, and excess *t*-BuNC (0.10 mL, 0.89 mmol) was added. The solution was stirred under a nitrogen atmosphere (0.5 h) at room temperature and then reduced to a small volume on a rotary evaporator. The solution was placed on a short silica gel column and eluted with CH_2Cl_2. The violet solution was collected, the solvents were removed on a rotary evaporator, and the product was crystallized from CH_2Cl_2/hexanes. The violet microcrystalline solid was filtered and washed with ice cold hexanes: yield 402 mg (97%); ^1H NMR (Table I); IR (Nujol) 1680 cm^{-1} ν_{CO}(amide), 1620 cm^{-1} ν_{CO}(amide), 2150 cm^{-1} $\nu_{C\equiv N}$. Anal. Calcd for $C_{43}H_{36}N_3O_4OsP·0.75(CH_2Cl_2)$: C, 55.69; H, 4.01; N, 4.45. Found: C, 55.60; H, 4.17; N, 4.43.

***cis*-β-Os(η^4-HBA-B)(dppe) (13).** *trans*-Os(η^4-HBA-B)$(PPh_3)_2$ (500 mg, 0.472 mmol) and diphenylphosphinoethane (200 mg, 2.36 mmol) were dissolved in dichloromethane (100 mL), and the solution was stirred overnight at room temperature. Ethanol was added, and the CH_2Cl_2 was removed on a rotary evaporator to produce a green solid. The solid was filtered and washed with a small portion of ice cold ethanol and hexanes: yield 359 mg (82%); ^1H NMR (Table I); ^{31}P NMR (Table II); IR (Nujol) 1660 cm^{-1} ν_{CO}(nonplanar amide); IR (Nujol) 1590 cm^{-1} ν_{CO}(planar amide). Anal. Calcd for $C_{46}H_{36}N_2O_4OsP_2$: C, 59.22; H, 3.89; N, 3.00. Found: C, 59.20; H, 3.89; N, 3.04.

***cis*-α-Os(η^4-CHBA-DCB)(*t*-Bupy)$_2$ (4).** *trans*-Os(η^4-CHBA-DCB)(*t*-Bupy)$_2$ (200 mg, 0.198 mmol) was electrooxidized by 1 Faraday per mol (1.42 V vs. Fc^+/Fc, CH_2Cl_2, 0.1 M TBAP). At room temperature, isomerization to the equilibrium mixture of isomers had occurred when the electrolysis was complete. The solution was cooled (-78 °C) and reduced with excess ferrocene dissolved in dichloromethane. The solvent volume was reduced on a rotary evaporator at room temperature, and the supporting electrolyte was precipitated with diethyl ether and collected by filtration. The procedure was repeated to ensure complete TBAP removal. Separation of the cis-α and trans isomers was achieved by column chromatography using silica gel (32–63 micron, Woelm, 150 g) and chlorobenzene/bromoethane (1:1 v/v) eluent. The front-running ferrocene band was collected and discarded. The next red band and the final dark band were separately collected, and the solvents were removed on a rotary evaporator. Both residues were recrystallized from CH_2Cl_2/hexane. The red compound was the pure cis-α isomer: yield 64 mg (74% based on K^+ = 1.3; 32% based on recovered osmium); ^1H NMR (Table III); IR (Nujol) 1645 cm^{-1} ν_{CO}(nonplanar amide) (br). Anal. Calcd for $C_{38}H_{32}N_4O_4OsCl_6·0.25(C_6H_{14})$: C, 45.92; H, 3.46; N, 5.42. Found: C, 45.90; H, 3.46; N, 5.42. The dark band proved to be a mixture of cis-α and trans isomers (1:2.6 by ^1H NMR: yield 75 mg (48% of **3** and 24% of **4** based on K^+ = 1.3; 38% based on recovered osmium).

***trans*-Os(η^4-CHBA-DCB)(*p*-MeOpy)$_2$ (3-MeO).** K_2[*trans*-Os(η^4-CHBA-DCB)$(O)_2$]·$4H_2O$ (300 mg, 0.350 mmol), triphenylphosphine (210 mg, 0.801 mmol), and *p*-methoxypyridine (4 mL, ca. 40 mmol) were dissolved in water (3 mL) and gently heated (20 min). After cooling, all volatiles were removed in vacuo. The residue was purified by twice precipitating it from THF with hexane. The precipitate was dissolved in THF (10 mL) and oxidized with excess bromine. After removal of the solvent on a rotary evaporator, the product was eluted through a short silica gel column with CH_2Cl_2 and recrystallized from CH_2Cl_2/hexane to yield a blue microcrystalline powder: yield 211 mg (63%); ^1H NMR (Table III). Anal. Calcd for $C_{32}H_{20}N_4Cl_6OsO_6·0.15(C_6H_{14})$: C, 40.64; H, 2.29; N, 5.76. Found: C, 40.61; H, 2.24; N, 5.74.

***trans*-Os(η^4-CHBA-DCB)(*p*-Etpy)$_2$ (3-Et).** K_2[*trans*-Os(η^4-CHBA-DCB)$(O)_2$]·$4H_2O$ (120 mg, 0.130 mmol), triphenylphosphine (85 mg, 0.324 mmol), and *p*-ethylpyridine (3.7 g, ca. 35 mmol) were dissolved in water (3 mL) and gently heated (45 min). After cooling, all volatiles were removed in vacuo. The residue was purified by twice precipitating it from THF with hexane. The precipitate was dissolved in THF (10 mL) and oxidized with bromine. After removal of the solvent on a rotary evaporator, the product was eluted through a short silica gel column with CH_2Cl_2 and recrystallized from CH_2Cl_2/hexane to yield a blue crystalline product: yield 60 mg (48%); ^1H NMR (Table III). Anal. Calcd for $C_{34}H_{24}N_4Cl_6OsO_4·0.2(C_6H_{14})$: C, 43.46; H, 2.78; N, 5.76. Found: C, 43.12; H, 2.84; N, 5.70.

***trans*-Os(η^4-CHBA-DCB)(*p*-Mepy)$_2$ (3-Me).** K_2[*trans*-Os(η^4-CHBA-DCB)$(O)_2$]·$4H_2O$ (120 mg, 0.130 mmol), triphenylphosphine (85 mg, 0.324 mmol), and *p*-picoline (3.8 g, ca. 41 mmol) were dissolved in water (3 mL) and gently heated (45 min). After cooling, all volatiles were removed in vacuo. The residue was purified by twice precipitating it from THF with hexane. The precipitate was dissolved in THF (25 mL) and oxidized with bromine. After removal of the solvent on a rotary evaporator, the product was eluted through a short silica gel column with CH_2Cl_2 and recrystallized from CH_2Cl_2/hexane to yield a dark blue crystalline solid. An analytical sample was obtained by purification on a preparatory TLC plate using toluene eluent followed by recrystallization from CH_2Cl_2/hexane: yield 74 mg (65%); ^1H NMR (Table III). Anal. Calcd for $C_{32}H_{20}N_4Cl_6OsO_4·0.3(C_6H_{14})$: C, 42.58; H, 2.56; N, 5.88. Found: C, 42.90; H, 2.44; N, 6.18.

***trans*-Os(η^4-CHBA-DCB)(*p*-Clpy)$_2$ (3-Cl).** K_2[*trans*-Os(η^4-CHBA-DCB)$(O)_2$]·$4H_2O$ (200 mg, 0.217 mmol), triphenylphosphine (140 mg, 0.534 mmol), and 4 mL of ca. 9.2 M *p*-chloropyridine solution in diethylether (ca. 37 mmol) were dissolved in water (2.5 mL) and gently heated (0.5 h). After cooling, all volatiles were removed in vacuo. The residue was purified by twice precipitating it from THF with hexane. The precipitate was dissolved in THF (25 mL) and oxidized with bromine. After removal of the solvent on a rotary evaporator, the product was

eluted through a silica gel column with CH_2Cl_2 and recrystallized from CH_2Cl_2/hexane to yield a dark blue microcrystalline powder: yield 143 mg (68%); ^1H NMR (Table III). Anal. Calcd for $C_{30}H_{14}N_4Cl_8OsO_4$: C, 37.21; H, 1.46; N, 5.79. Found: C, 37.28; H, 1.61; N, 5.71.

***trans*-Os(η^4-CHBA-DCB)(*p*-Brpy)$_2$ (3-Br).** K_2[*trans*-Os(η^4-CHBA-DCB)(O)$_2$]·4H_2O (120 mg, 0.130 mmol), triphenylphosphine (85 mg, 0.324 mmol), and 2.7 mL of ca. 8.8 M *p*-bromopyridine solution in diethyl ether (ca. 24 mmol) were dissolved in water (1.8 mL) and gently heated (0.5 h). After cooling, all volatiles were removed in vacuo. The residue was purified by twice precipitating it from THF with hexane. The precipitate was dissolved in THF (25 mL) and oxidized with bromine. After removal of the solvent on a rotary evaporator, the product was eluted through a silica gel column with CH_2Cl_2/10% THF and recrystallized from CH_2Cl_2/hexane to yield a dark blue crystalline product: yield 65 mg (47%); ^1H NMR (Table III). Anal. Calcd for $C_{30}H_{14}N_4Br_2Cl_6OsO_4$: C, 34.08; H, 1.33; N, 5.30. Found: C, 34.34; H, 1.58; N, 5.10.

***trans*-Os(η^4-CHBA-DCB)(*p*-Acpy)$_2$ (3-Ac).** K_2[*trans*-Os(η^4-CHBA-DCB)(O)$_2$]·4H_2O (120 mg, 0.130 mmol), triphenylphosphine (85 mg, 0.324 mmol), and *p*-acetylpyridine (4.4 g, 36 mmol) were dissolved in water (3 mL) and gently heated (1 h). After cooling, all volatiles were removed in vacuo. The residue was purified by twice precipitating it from THF with hexane. The precipitate was dissolved in THF (25 mL) and oxidized with bromine. After removal of the solvent on a rotary evaporator, the product was eluted through a silica gel column with excess CH_2Cl_2 and recrystallized from CH_2Cl_2/hexane to yield a dark blue-green crystalline solid: yield 73 mg (57%); ^1H NMR (Table III). Anal. Calcd for $C_{34}H_{20}N_4Cl_6OsO_6$·0.1(C_6H_{14}): C, 41.89; H, 2.17;, N, 5.65. Found: C, 42.00; H, 2.21; N, 5.67.

***cis*-β-Os(η^4-CHBA-DCB)(*t*-BuNC)$_2$ (5).** *cis*-α-Os(η^4-CHBA-DCB)(*t*-BuNC)$_2$ (15 mg, 15 μmol) was electroreduced by 2 Faradays per mol at −1.20 V vs. Fc^+/Fc during which the solution turned green. The solution was reoxidized by 2 Faradays per mol, and diethyl ether was added (ca. 300 mL) to precipitate the supporting electrolyte. After filtration, the solvent was removed on a rotary evaporator, and the product was eluted through a silica gel column with excess CH_2Cl_2/1% THF. Recrystallization from CH_2Cl_2/hexane afforded a green microcrystalline product: yield 12 mg (80%); ^1H NMR (Table III); IR (Nujol) 1694 cm^{-1} ν_{CO}(nonplanar amide), 1622 cm^{-1} ν_{CO}(planar amide), 2154 cm^{-1} $\nu_{C\equiv N}$, 2002 cm^{-1} $\nu_{C\equiv N}$.

***cis*-α-Os(η^4-CHBA-DCB)(bipy) (12).** *trans*-Os(η^4-CHBA-DCB)(PPh_3)$_2$ (400 mg, 0.316 mmol) and 2,2′-dipyridyl (800 mg, 5.12 mmol) were dissolved in toluene (25 mL) and heated under reflux (0.5 h) during which time the color darkened. The cooled solution was eluted through a silica gel column with excess CH_2Cl_2. Three bands separated: a front running green band, a red band, and finally a black band. The green material was isolated and recrystallized from CH_2Cl_2/hexane. It proved to be unreacted starting material (67 mg). Isolation of the red material followed by recrystallization from CH_2Cl_2/hexane afforded red microcrystalline product: yield 59 mg (25%; adjusted for recovered starting material); ^1H NMR (Table III); IR (Nujol) 1631 cm^{-1} ν_{CO}(nonplanar amide). Anal. Calcd for $C_{30}H_{14}Cl_6N_4O_4Os$·0.33(C_6H_{14}): C, 41.79; H, 2.03; N, 6.05. Found: C, 41.75; H, 2.07; N, 5.98.

***cis*-β-Os(η^4-CHBA-DCB)(bipy) (11).** The final black material off the column in the previous synthesis was isolated and recrystallized from CH_2Cl_2/hexane to afford a black microcrystalline product: yield 12.5 mg (5.3%; adjusted for recovered starting material); ^1H NMR (Table III); IR (Nujol) 1635 cm^{-1} ν_{CO}(nonplanar amide), 1622 cm^{-1} ν_{CO}(planar amide). Anal. Calcd for $C_{30}H_{14}Cl_6N_4O_4Os$: C, 40.15; H, 1.57; N, 6.24. Found: C, 40.44; H, 1.74; N, 6.25.

***cis*-β-Os(η^4-CHBA-DCB)(dppe) (14).** *trans*-Os(η^4-CHBA-DCB)(PPh_3)$_2$ (80 mg, 0.063 mmol) and diphenylphosphinoethane (35 mg, 0.413 mmol) were dissolved in benzene (10 mL) and heated under reflux (15 min). The solution color remained green during heating. After cooling, the solvent was removed on a rotary evaporator. The resulting residue was eluted through a short silica gel column with excess CH_2Cl_2 and recrystallized from CH_2Cl_2/hexane to yield a green crystalline product: yield 67 mg (93%); ^1H NMR (Table III); ^{31}P NMR (Table II); IR (Nujol) 1670 cm^{-1} ν_{CO}(nonplanar amide); 1608 cm^{-1} ν_{CO}(planar amide). Anal. Calcd for $C_{46}H_{30}Cl_6N_2O_4OsP_2$·0.5($C_6H_{14}$): C, 49.76; H, 3.15; N, 2.37. Found: C, 49.64; H, 3.10; N, 2.36.

***trans*-Os(η^4-CHBA-DCB)($OPPh_3$)$_2$ (15).** *trans*-Os(η^4-CHBA-DCB)(PPh_3)$_2$ (511 mg, 0.404 mmol) was dissolved in chloroform (50 mL), and iodosylbenzoic acid (1.1 g, 8.03 mmol) was added which did not dissolve. The two phase system was stirred and heated (60 °C, 1.5 h) during which the solution turned from green to red. The solution was cooled and filtered, methanol (150 mL) was added, and solvent was removed on a rotary evaporator until a precipitate started to appear. After 5 h at 5 °C, the solvent volume was reduced (to ca. 25 mL), and filtration yielded a black crystalline product: yield 477 mg (91%); ^1H NMR (Table III); ^{31}P NMR (Table II); IR (Nujol) 1608 cm^{-1} ν_{CO}(planar amide). Anal. Calcd for $C_{56}H_{36}Cl_6N_2O_6OsP_2$: C, 51.83; H, 2.80; N, 2.16. Found: C, 51.86, H, 2.92; N, 2.18.

Mixture of *trans*- and *cis*-α-[Os(η^4-CHBA-DCB)($OPPh_3$)$_2$][PF_6] (15$^+$ and 16$^+$). *trans*-Os(η^4-CHBA-DCB)($OPPh_3$)$_2$ (30 mg, 0.023 mmol) was dissolved in dichloromethane (5 mL), and excess solid nitrosonium hexafluorophosphate was added which did not dissolve. The solution was sealed with a septum and stirred at room temperature (0.5 h) during which the solution turned from red to purple indicative of product formation. The purple solution was filtered away from unreacted [NO][PF_6], and the solvent was removed in vacuo affording deep purple crystalline product: yield 30 mg (96%); IR (KBr) 1680 cm^{-1} ν_{CO}(nonplanar amide) (cis-α-isomer); 1605 cm^{-1} ν_{CO}(planar amide) (trans isomer). Anal. Calcd for $C_{56}H_{36}Cl_6F_6N_2O_6OsP_3$·$H_2O$ (solvate was not quantified): C, 46.05; H, 2.62; N, 1.92. Found: C, 46.08; H, 2.57; N, 1.95.

Mixture of *trans*- and *cis*-α-Os(η^4-CHBA-DCB)($OPPh_3$)$_2$ (15) and (16). *trans*-Os(η^4-CHBA-DCB)($OPPh_3$)$_2$ (150 mg, 0.116 mmol) was dissolved in dichloromethane (15 mL), and excess solid nitrosonium hexafluorophosphate was added which did not dissolve. After the solution stirred at room temperature (15 min), the resulting purple solution was filtered away from unreacted [NO][PF_6], cooled (−78 °C), and reduced with ferrocene (1.5 equiv). In a walk-in cold room (5 °C) the material was flash chromatographed through silica gel (250 g) with precooled dichloromethane. The front-running ferrocene band was collected and discarded. The subsequent red band was collected and crystallized from CH_2Cl_2/hexane at −20 °C to yield a red powder. The ^1H NMR of this material revealed it to be a 3:1 mixture of cis-α and trans isomers: yield 90.2 mg (60% based on recovered osmium); ^1H NMR (Table III); IR (Nujol) 1626 cm^{-1} ν_{CO}(nonplanar amide) (br).

Results and Discussion

Thermodynamic Studies of Trans ⇌ Cis-α Equilibrium Processes. The cyclic voltammogram of *trans*-Os(η^4-**1**)(*t*-Bupy)$_2$, **3**,[4,15] is shown in Figure 1a. The CV shown in Figure 1b is obtained following room temperature controlled-potential electrooxidation of **3** by 1 Faraday per mol. The oxidation produces a mixture of **3**$^+$ and a new compound **4**$^+$, as indicated by the appearance of a new set of waves. The peak currents for the couples associated with **3** in Figure 1a equal the sum of the peak currents associated with **3**$^+$ and **4**$^+$ in Figure 1b; hence, material balance is maintained. Compound **4**$^+$ is the cis-α diastereomer of **3**$^+$ (vide infra, Figure 2).[16] If this mixture is rapidly reduced by addition of excess ferrocene at −78 °C, a stable solution of **3** and **4** is formed which can be separated by column chromatography on silica gel with a chlorobenzene/bromoethane (1:1) eluent. Electrooxidation of **3** or **4** by 1 Faraday per mol at −78 °C affords pure solutions of

(15) A bispyridine analogue of *trans*-**1** has been characterized by X-ray crystallography.

(16) The nomenclature for the three arrangements of a tetradentate ligand upon an octahedral metal center has been defined previously: Sargeson, A. M.; Searle, G. H. *Nature (London)* **1963**, *200*, 356–357.

Table III. ^{1}H NMR Data for all Compounds of PAC Ligand [η^4-CHBA·DCB]$^{4-}$, 1[a]

	chelate ligand												other	
	CHBA				DCB		H_o	H_m	other py					
									pyridine					
trans-Os(η^4-I)(*p*-Clpy)$_2$, **3·Cl**[b]	10.34 2 H, d $J_{m,m'} = 3$[d]	9.77 2 H, d			7.26 2 H, s		−7.37 4 H, d $J_{o,m} = 7$	8.21 4 H, d						
trans-Os(η^4-I)(*p*-Brpy)$_2$, **3·Br**[b]	10.34 2 H, d $J_{m,m'} = 3$	9.79 2 H, d			7.36 2 H, s		−7.52 4 H, d $J_{o,m} = 7$	8.42 4 H, d						
trans-Os(η^4-I)(*p*-Mepy)$_2$, **3·Me**[b]	11.01 2 H, d $J_{m,m'} = 3$	9.71 2 H, d			7.36 2 H, s		−8.01 4 H, d $J_{o,m} = 7$	7.88 4 H, d	10.70 6 H, s, (CH_3)					
trans-Os(η^4-I)(*p*-Etpy)$_2$, **3·Et**[b]	11.05 2 H, d $J_{m,m'} = 3$	9.84 2 H, d			7.57 2 H, s		−8.49 4 H, d $J_{o,m} = 7$	7.74 4 H, d	9.96 4 H, q, (CH_2) $J = 8$	−0.16 6 H, t, (CH_3)				
trans-Os(η^4-I)(*p*-MeOpy)$_2$, **3·MeO**[b,e]	11.55 2 H, d $J_{m,m'} = 3$	9.96 2 H, d			7.70 2 H, s		−8.48 4 H, d $J_{o,m} = 6$	6.33 4 H, d	4.07 6 H, s, (OCH_3)					
trans-α-Os(η^4-I)(*t*-Bupy)$_2$, **3-*t*-Bu**[c,e]	11.10 2 H, d $J_{m,m'} = 3$	9.79 2 H, d			7.50 2 H, s		−8.48 4 H, d $J_{o,m} = 7$	7.96 4 H, d	0.07 18 H, s, ($C(CH_3)_3$)					
cis-α-Os(η^4-I)(*t*-Bupy)$_2$, **4-*t*-Bu**[c,d,g]	7.73 2 H, d $J_{m,m'} = 3$	7.23 2 H, d			7.91 2 H, s		7.98 2 H, d 7.82 2 H, d $J_{o,m} = J_{o',m'} = 6$	7.66 2 H, dd 7.40 2 H, dd	1.27 18 H, s, ($C(CH_3)_3$) $J_{m,m'} = 2$					
trans-Os(η^4-I)(*p*-Acpy)$_2$, **3·Ac**[c]	10.03 2 H, d $J_{m,m'} = 3$	9.28 2 H, d			6.78 2 H, s		−5.63 4 H, d $J_{o,m} = 7$	9.45 4 H, d	1.45 6 H, s, (CH_3)					
													t-Bu	
cis-α-Os(η^4-I)(*t*-BuNC)$_2$, **5**[b]	7.43 2 H, d $J_{m,m'} = 3$	8.42 2 H, d			8.39 2 H, s								1.44 18 H, s	
cis-β-Os(η^4-I)(*t*-BuNC)$_2$, **6**[b]	7.44 2 H, br	7.82 2 H, br			9.79 1 H, br	5.77 1 H, br							1.44 9 H, s	1.22 9 H, s
cis-α-Os(η^4-I)(bipy), **12**[b]	8.20 2 H, d	7.11 2 H, d			8.28 2 H, s		7.96 1 H $J_{o,m} = 5.6$ $J_{o,p} = 1.2$	7.56 1 H $J_{m,p} = J_{m',p} = 7.8$ $J_{m,m'} = 0.9$	7.81 1 H, (H_p)	8.58 1 $H_{m'}$ H				
cis-β-Os(η^4-I)(bipy), **11**[b,f]	10.13 1 H, d $J_{m,m'} = 3$	6.77 1 H, d	7.63 1 H, d	7.57 1 H, d	7.80 1 H, s	3.19 1 H, s	−2.97 1 H, d −12.47 1 H, d $J_{o,m} \approx 5.6$	10.40 1 H, dd 10.91 1 H, dd $J_{m,p} \approx 7.0$	6.59 1 H, dd (H_p) −2.28 1 H, dd, (H_p) $J_{m',p} \approx 8.0$	9.57 1 H, d, ($H_{m'}$) 8.83 1 H, d, ($H_{m'}$)				

	Phosphine Aromatic							dppe Aliphatic			
						H_o	H_m	H_p			
cis-β-Os(η^4-1)(dppe), 14[c,d]	7.20	7.09	7.01	6.96	10.29	5.19	7.55	7.87	7.43	4.28	3.95	3.42	2.10
	1 H, d	1 H, d	1 H, d	1 H, d	1 H, s	1 H, s	2 H, d	2 H, m	1 H, t	1 H, br	1 H, br	1 H, br	1 H, br
	$J_{m,m'} = 3$						6.63	7.09	7.29				
							2 H, dd	2 H, dd	1 H, t				
							6.79	7.36	7.23				
							4 H, dd	2 H, dd	2 H, t				
								7.34					
								2 H, dd					
							$J_{o,p} \approx J_{o,m} \approx 8$	$J_{m,p} \approx 7$					
cis-α-Os(η^4-1)($OPPh_3$)$_2$, 16[b,d,h]	7.08	6.89			6.82		7.36	7.70	7.63				
	2 H, d	2 H, d			2 H, s		12 H, ddd	12 H, br	6 H, t				
	$J_{m,m'} = 3$						$J_{o,p} = J_{o,m} = 8$						
							$J_{o,p} = 3$	$J_{m,p} = 7$					
trans-Os(η^4-1)($OPPh_3$)$_2$, 15[b]	9.76	10.53			8.91		5.52	7.45	7.28				
	2 H, d	2 H, d			2 H, s		12 H, ddd	12 H, ddd	6 H, dt				
	$J_{m,m'} = 3$						$J_{o,p} = 13.1$	$J_{m,p} = 3.5$	$J_{o,m} = 8$				
							$J_{o,p} = 1.2$	$J_{m,p} = 7.5$					

[a] The chemical shifts of paramagnetic osmium(IV) species are somewhat concentration dependent. Measured at 400 MHz. [b] δ in $CDCl_3$. [c] δ in CD_2Cl_2. [d] Coupled protons established by decoupling experiments; *J* values in Hz. [e] Measured at 90 MHz. [f] Resonance assignment from JCOSY experiment. [g] Spectrum measured at −50 °C. At low temperature, pyridine rotation is hindered; $\Delta G^{\ddagger} \approx 13 \pm 1$ kcal·mol^{-1} at 0 °C, determined by variable temperature NMR measurements.[29] [h] Spectrum measured at −20 °C.

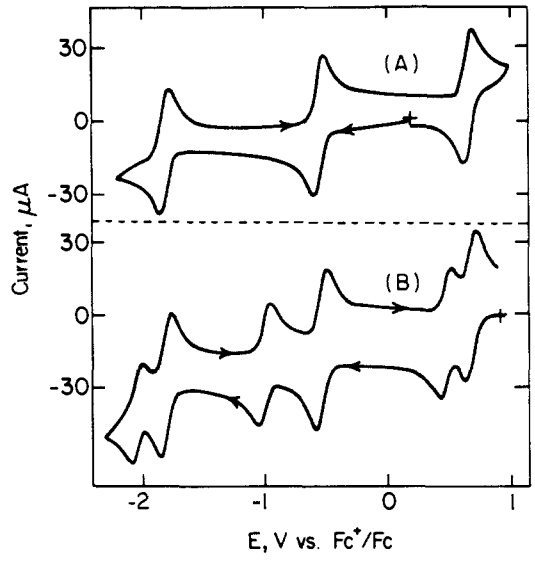

Figure 1. Cyclic voltammograms of 4.1 mM **3** in CH_2Cl_2, 0.1 M TBAP at 0.03 cm^2 Pt electrode. Scan rate = 200 mV·s^{-1}: (A) osmium(IV) and (B) monocation stage.

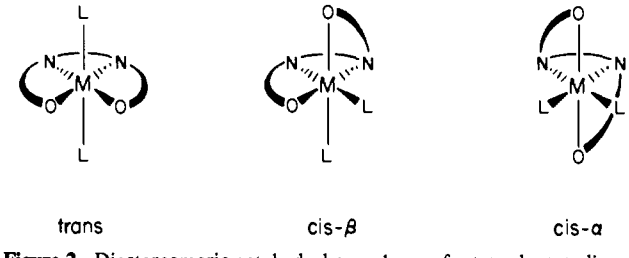

Figure 2. Diastereomeric octahedral complexes of a tetradentate ligand and two identical monodentate ligands.

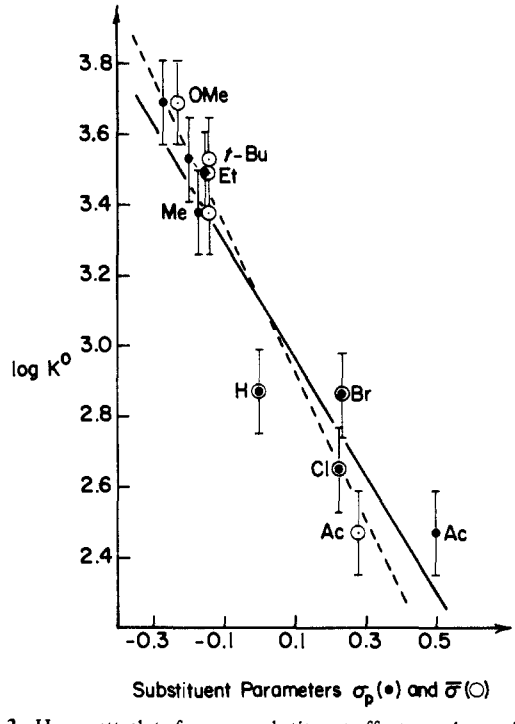

Figure 3. Hammett plots for para substituent effects on the equilibrium *cis*-α-Os(η^4-**1**)(*p*-X-py)$_2$ ⇌ *trans*-Os(η^4-**1**)(*p*-X-py)$_2$. Data measured in CH_2Cl_2 at 295 ±2 K.

3^+ and 4^+ (determined by CV). Isomerization occurs upon warming each solution to room temperature and identical distributions of 3^+ and 4^+ are produced, each displaying a CV identical with that of Figure 1b. Hence, 3^+ and 4^+ are in equilibrium at room temperature. If it is assumed that 3^+ and

Table IV. Formal Potentials and Equilibrium Constants for Os(η^4-**1**)(*p*-X-py)$_2$ Complexes[a]

		formal potentials			formal potentials			formal potentials		
p-X-	K^+	cis-α	trans	K^0	cis-α	trans	K^-	cis-α	trans	K^{2-}
Ac-	0.37 ± 0.02	+0.58	+0.75	3.0×10^2 ±0.8×10^2	−0.83	−0.32	1.5×10^{11} ±0.4×10^{11}	−1.46	−1.30	8.1×10^{13} ±3.2×10^{13}
Cl-	0.83 ± 0.02	+0.58	+0.74	4.5×10^2 ±1.3×10^2	−0.89	−0.39	1.6×10^{11} ±0.6×10^{11}	−1.81	−1.59	8.8×10^{14} ±4.3×10^{14}
Br-	0.90 ± 0.02	+0.58	+0.75	7.2×10^2 ±2.0×10^2	−0.89	−0.38	3.7×10^{11} ±1.7×10^{11}	*b*	−1.56	
H-	0.62 ± 0.02	+0.54	+0.72	7.4×10^2 ±2.1×10^2	−0.92	−0.44	1.2×10^{11} ±0.5×10^{11}	−1.89	−1.68	4.5×10^{14} ±2.2×10^{14}
Me-	0.62 ± 0.02	+0.49	+0.70	2.4×10^3 ±0.7×10^3	−0.97	−0.50	7.5×10^{11} ±1.0×10^{11}	−1.99	−1.78	9.8×10^{14} ±4.7×10^{14}
Et-	1.20 ± 0.05	+0.49	+0.69	3.1×10^3 ±0.9×10^3	−0.98	−0.52	2.2×10^{11} ±0.9×10^{11}	−2.00	−1.78	1.3×10^{15} ±0.6×10^{15}
t-Bu-	1.30 ± 0.05	+0.50	+0.70	3.4×10^3 ±0.9×10^3	−0.97	−0.51	2.4×10^{11} ±0.9×10^{11}	−2.00	−1.78	2.0×10^{15} ±1.0×10^{15}
MeO-	0.85 ± 0.02	+0.45	+0.67	4.9×10^3 ±1.4×10^3	−1.00	−0.55	2.4×10^{11} ±0.9×10^{11}	*b*	*b*	

[a] Electrochemical data measured in CH_2Cl_2/0.1 M TBAP at 22 ± 1 °C and referenced to Fc^+/Fc internal standard (V). [b] Irreversible couple.

4$^+$ have similar diffusion coefficients, then limiting currents from normal pulse voltammetry can be used to calculate the equilibrium concentration ratio. The equilibrium constant for the **4**$^+$ ⇌ **3**$^+$ equilibrium, K^+, is 1.3 at 22 °C.[17]

The formal potentials for the two diastereomers together with K^+ can be used to derive the equilibrium constants for the cis-α ⇌ trans isomerizations at the osmium(IV), -(III), and -(II) oxidation states, K^0, K^-, and K^{2-}, respectively, as described in the Experimental Section (Scheme I). Note that K^0 is 3.4×10^3 in favor of the trans isomer. This indicates that **4**, obtained in the ferrocene reduction, is thermodynamically unstable. Compound **4** does indeed revert to **3** upon warming ($t_{1/2} = 2.7 \times 10^4$ s in 1,2-dichloroethane at 60 °C).[18,19] Note also that the cis-α ligand complement becomes increasingly favored as the complex becomes more oxidized as indicated by the trend in the equilibrium constants in Scheme I. This suggests that the cis-α complement is more donating than the trans complement. Apparently electronic demands at the metal center affect the equilibria. We wished to assess the influence of electronic factors.

One approach to quantifying the role of electronic factors in equilibrium processes is to search for linear free energy relationships.[20a,b] In such a study, an experimental rate constant (k) or equilibrium constant (K) is correlated, as some chosen substituent is varied, with a substituent constant, σ, that has been predetermined by employing the Hammett equation for a related parent system.

$$\log(k/k_0) = \rho\sigma \text{ or } \log(K/K_0) = \rho\sigma$$

A good correlation shows that the system being studied responds to the electronic properties of the substituents as some linear function of the response of the parent system, suggests that

Scheme I

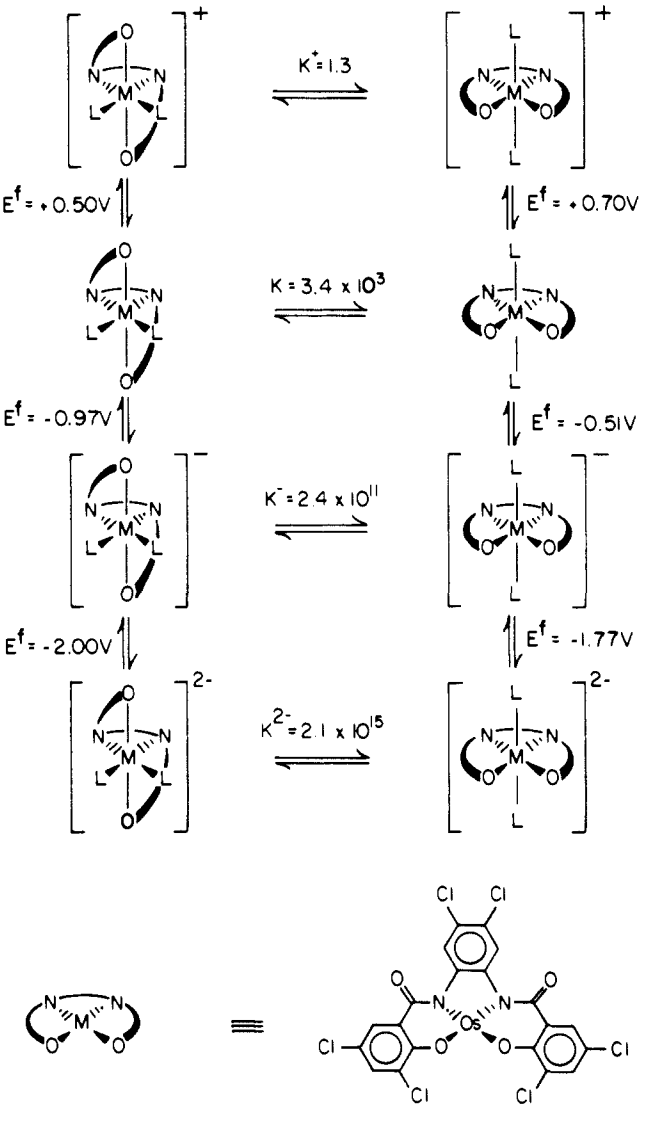

(17) Bard, A. J.; Faulkner, L. F. *Electrochemical Methods. Fundamentals and Applications*; Wiley: New York, 1980; pp 186–199.

(18) For examples of studies of interconversions of diastereomeric complexes induced by redox processes, see: (a) Gaudiello, J. G.; Wright, T. C.; Jones, R. A.; Bard, A. J. *J. Am. Chem. Soc.* **1985**, *107*, 888. (b) Datta, S.; Dezube, B.; Kouba, J. K.; Wreford, S. S. *J. Am. Chem. Soc.* **1978**, *100*, 4404–4412. (c) Lewis, J.; Whyman, R. *J. Chem. Soc.* **1965**, 5486–5491. (d) Crossing, P. F.; Snow, M. R. *J. Chem. Soc. A* **1971**, 610–612. (e) Reiman, R. H.; Singleton, E. *J. Organomet. Chem.* **1971**, *32*, C44–C46. (f) Johnson, B. F. G.; Bhaduri, S.; Connelly, N. G. *J. Organomet. Chem.* **1972**, *40*, C36–C38. (g) George, T. A.; Siebold, C. D. *Inorg. Chem.* **1973** *12*, 2458–2552. (h) Wimmer, F. L.; Snow, M. R.; Bond, A. M. *Inorg. Chem.* **1974**, *13*, 1617–1623. (i) Bond, A. M.; Colton, R.; Jackowski, J. J. *Ibid.* **1975**, *14*, 274–278. (j) Bond, A. M.; Colton, R.; Jackowski, J. J. *Ibid.* **1975**, *14*, 2526–2530. (k) Bond, A. M.; Colton, R.; McCormick, M. J. *Ibid.* **1977**, *16*, 155–159. (l) Bond, A. M.; Grabaric, B. S.; Grabaric, Z. *Ibid.* **1978**, *17*, 1013–1018. (m) Bond, A. M.; Colton, R.; Jackowski, J. J. *Ibid.* **1978**, *17*, 2153–2160. (n) Bond, A. M.; Colton, R.; McDonald, M. E. *Ibid.* **1978**, *17*, 2842–2847. (o) Bond, A. M.; Keene, F. R.; Rumble, N. W.; Searle, G. H.; Snow, M. R. *Ibid.* **1978**, *17*, 2847–2853. (p) Connor, J. A.; Riley, P. I.; Rix, C. J. *J. Chem. Soc., Dalton Trans.* **1977**, 1317–1323. Connor, J. A.; Riley, P. I. *J. Chem. Soc., Dalton Trans.* **1979**, 1231–1237. (q) Connor, J. A.; Riley, P. I. *Ibid.* **1979**, 1318.

(19) Alternatively, **4** can be rapidly converted to **3** at room temperature by addition of a trace of **3**$^+$ or **4**$^+$. These cations catalyze the isomerization processes by cycling the neutral compounds through the monocation stage where the isomerizations are fast.

(20) (a) Johnson, C. D. *The Hammett Equation*; Cambridge University Press: Cambride, 1973. (b) Lowry, T. H.; Richardson, K. S. *Mechanism and Theory in Organic Chemistry*, 2nd ed.; Harper & Row: New York, 1981; pp 130–145. (c) Substituent parameters taken from Gordon, A. J.; Ford, R. A. *The Chemists Companion*; Wiley: New York, 1972; pp 144–155.

Table V. ρ Values for Correlations of Formal Potentials with σ

couple	ρ	r
trans-monocation/osmium(IV)	2.39	0.97
cis-α-monocation/osmium(IV)	4.08	0.98
trans-osmium(IV/III)	5.91	0.98
cis-α-osmium(IV/III)	3.94	0.98
trans-osmium(III/II)	9.17	0.99
cis-α-osmium(III/II)	9.17	0.99

perturbations induced by other parameters are minimal, and provides information about the sensitivity of the response relative to the parent system. The sensitivities are reflected in the ρ values, i.e., the slopes of the linear relationships. Because the Hammett equation is a single equation in two variables, all systems relate back to substituted benzoic acid dissociations for which the original σ values were obtained by arbitrarily setting ρ at 1. In the current study the series of complexes *trans*-Os(η^4-**1**)(*p*-X-py)$_2$, **3-X** (X = MeO, Et, Me, H, Cl, Br, and CH_3CO), were synthesized (Scheme II), the formal potentials were measured, and the equilibrium data were derived for each for use in the correlations described below (see Table IV).

The log K^0 values were plotted against a variety of substituent parameters.[20c] The best fits at the osmium(IV) stage were found for the substituent parameters σ_p ($\rho = -1.6$, $r = 0.95$, Figure 3) and Fischer $\bar{\sigma}$ (the substituent parameter for pyridinium ion dissociations, $\rho = -2.1$, $r = 0.95$, Figure 3).[21a,b] The existence of these admittedly rather poor relationships supports the suggestion that K^0 responds to electronic effects.[22]. As the ancillary pyridine ligands become less donating, the equilibrium favors the more donating cis-α ligand complement. Since two pyridine ligands are involved in the isomerization reactions, $\rho/2$ is a more appropriate measure of the relative sensitivities. The $\rho/2$ value of −1.05, found for the correlation with $\bar{\sigma}$, is considerably smaller in magnitude than that for the correlation of pyridinium acid dissociation constants to $\bar{\sigma}$ (6.01)[21a] but very similar to the ρ value for benzoic acid dissociations. In contrast to the pyridinium ion and benzoic acid deprotonations, no charge change accompanies the isomerization processes, a possible reason for the reduced sensitivity relative to the pyridinium ion dissociations.

No linear relationship was found for the monocation stage. Correlations were not sought for the osmium(III) or osmium(II) equilibrium constants, because the propagated errors associated with the data were considered too large for such correlations to be meaningful.[23]

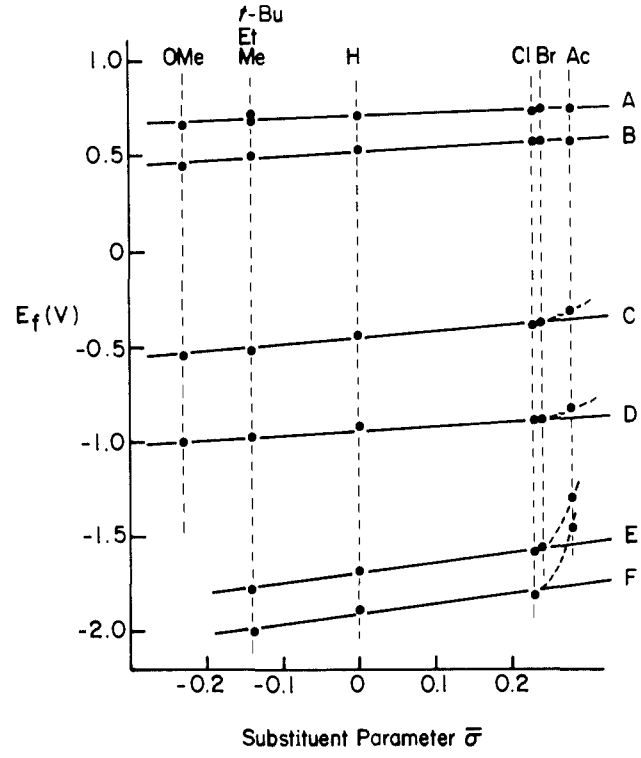

Figure 4. Plots of formal potentials vs. Fischer $\bar{\sigma}$ substituent parameters[21a] for Os(η^4-**1**)(*p*-X-py)$_2$. Data measured in CH_2Cl_2 at 295 ±2 K: (A) *trans*-monocation/osmium(IV) formal potentials, slope = 0.14, r = 0.97; (B) *cis*-α-monocation/osmium(IV) couple, slope = 0.239, r = 0.98; (C) *trans*-osmium(IV/III) formal potentials, slope = 0.35, r = 0.98;† (D) *cis*-α-osmium(IV/III) formal potentials, slope = 0.23, r = 0.98;† (E) *trans*-osmium(III/II) formal potentials, slope = 0.54, r = 0.99;† (F) *cis*-α-osmium(III/II) formal potentials, slope = 0.54, r = 0.99;† The † stands for datum for the *p*-Acpy system not included in correlation.

The isomerization processes are affected in other ways by the nature of the ancillary monodentate ligands. CV and controlled potential electrooxidation studies reveal that *trans*-[Os(η^4-**1**)-(PPh_3)$_2$]$^+$ is the only isomer formed upon oxidation of the osmium(IV) precursor at room temperature. Presumably steric factors disfavor cis phosphine ligands.

In Figure 4 the formal potentials for all the various couples are plotted against the $\bar{\sigma}$ substituent constants. The data correlate well for the IV/III and III/II formal potentials with the exception of the *p*-acetylpyridine data. When the formal potential data are converted to log K values for the equilibria

$$[\mathrm{Os}(\eta^4\text{-}\mathbf{1})(p\text{-X-py})_2]^n + \mathrm{Fc} \rightleftharpoons [\mathrm{Os}(\eta^4\text{-}\mathbf{1})(p\text{-X-py})_2]^{n-1} + \mathrm{Fc}^+$$

the derived $\rho/2$ values are found to lie in the range of 1.19–4.58, signaling a moderate to substantial sensitivity of the equilibria to the electronic effects of the pyridine substituents (Table V). Note that the formal potentials for the *p*-acetylpyridine system lie on the line for the monocation/osmium(IV) couples but deviate from the line with increasing magnitude as the oxidation states are lowered. The deviation implies that the acetyl substituents exert a much larger electron-withdrawing effect in the redox processes than in the dissociation of pyridinium ions relative to that expected from the behavior of the other pyridine ligands.

N-aromatic heterocycles have been described as being a general class of moderately strong π-acids,[24a] and persuasive arguments

(21) (a) Fischer, A.; Galloway, W. J.; Vaughan, J. *J. Chem. Soc.* **1964**, 3591–3596. (b) For a recent treatment of the relative field/inductive and resonance contributions, see: Taagepera, M.; Summerhays, K. D.; Hehre, W. J.; Topsom, R. D.; Pross, A.; Radom, L.; Taft, R. W. *J. Org. Chem.* **1981**, *46*, 891–903.

(22) Hammett plots have been derived for other inorganic equilibrium processes involving pyridine ligands. For instance, a ρ value of −1.64 was found for $\bar{\sigma}$ correlation with the equilibrium constants for the replacement of piperidine by parasubstituted pyridines in an alkyl(piperidine)cobaloxime complex in chloroform at 25 °C.[22a] The ρ values of −1.50,[22b] −2.2,[22c] and −3.1[22c] were found for the σ_p correlations with the stability constants in benzene at 25 °C for formation of pyridine adducts of zinc, cadmium, and mercury tetraphenylporphyrin complexes, respectively. When the Imai et al. correlation of pyridine basicity with the binding constants of parasubstituted pyridine ligands to *meso*-[tetrakis[α^4-2-((neopentylcarbonyl)amino)phenyl]-porphyrinato]cobalt(II) at 25 °C in toluene is converted to a correlation with $\bar{\sigma}$, a ρ value of −1.38 (r = 0.99) is found.[22d] Similarly, ρ values of −2.25 (r = 0.99) and −4.62 (r = 0.98) have been derived from Jones and Twigg's data for the correlation with $\bar{\sigma}$ of the first and second binding constants, respectively, of parasubstituted pyridine ligands to iron(II) phthalocyanine in Me_2SO at 25 °C.[22e] While the ρ value found of −2.1 for the isomerization process studied in this work lies in the general range of the values for ligand binding equilibria, any comparisons are limited by the different natures of the processes involved. It should also be noted that two pyridine ligands are involved in the isomerization systems. (a) Jensen, F. R.; Kiskis, R. C. *J. Am. Chem. Soc.* **1975**, *97*, 5820–5825. (b) Kirksey, C. H.; Hambright, P.; Storm, C. B. *Inorg. Chem.* **1969**, *8*, 2141–2144; ρ value reported as +1.50. (c) Kirksey, C. H.; Hambright, P. *Inorg. Chem.* **1970**, *9*, 958–960; positive ρ values reported. (d) Imai, H.; Nakata, K.; Nakatsubo, A. *Synth. React. Inorg. Met.-Org. Chem.* **1983**, *13*, 761–780. (e) Jones, J. G.; Twigg, M. V. *Inorg. Chim. Acta* **1974**, *10*, 103–108. All data were employed for correlation with first binding constants. The second binding constant for *p*-cyanopyridine was omitted from the correlation because the datum deviates significantly from the otherwise good linear relationship for log K_2 vs. pK_{BH^+}.

(23) The major error component in the equilibrium data comes from the confidence limits in the formal potentials (±5 mV). Thus, over the range of pyridine complexes investigated, for K^0 the error depends on σ_{K^+} by 0.6–3.5%, on σ_{E^f} by 94–97%, and on σ_T by 2.3–4.2%; for K^{-1} the error depends on σ_{K^+} by 0.3–1.6%, on σ_{E^f} by 87–89%, and on σ_T by 10.2–11.8%; and for K^{-2} the error depends on σ_{K^+} by 0.2–1.1%, on σ_{E^f} by 90–91%, and on σ_T by 8.3–9.0%.

Scheme II

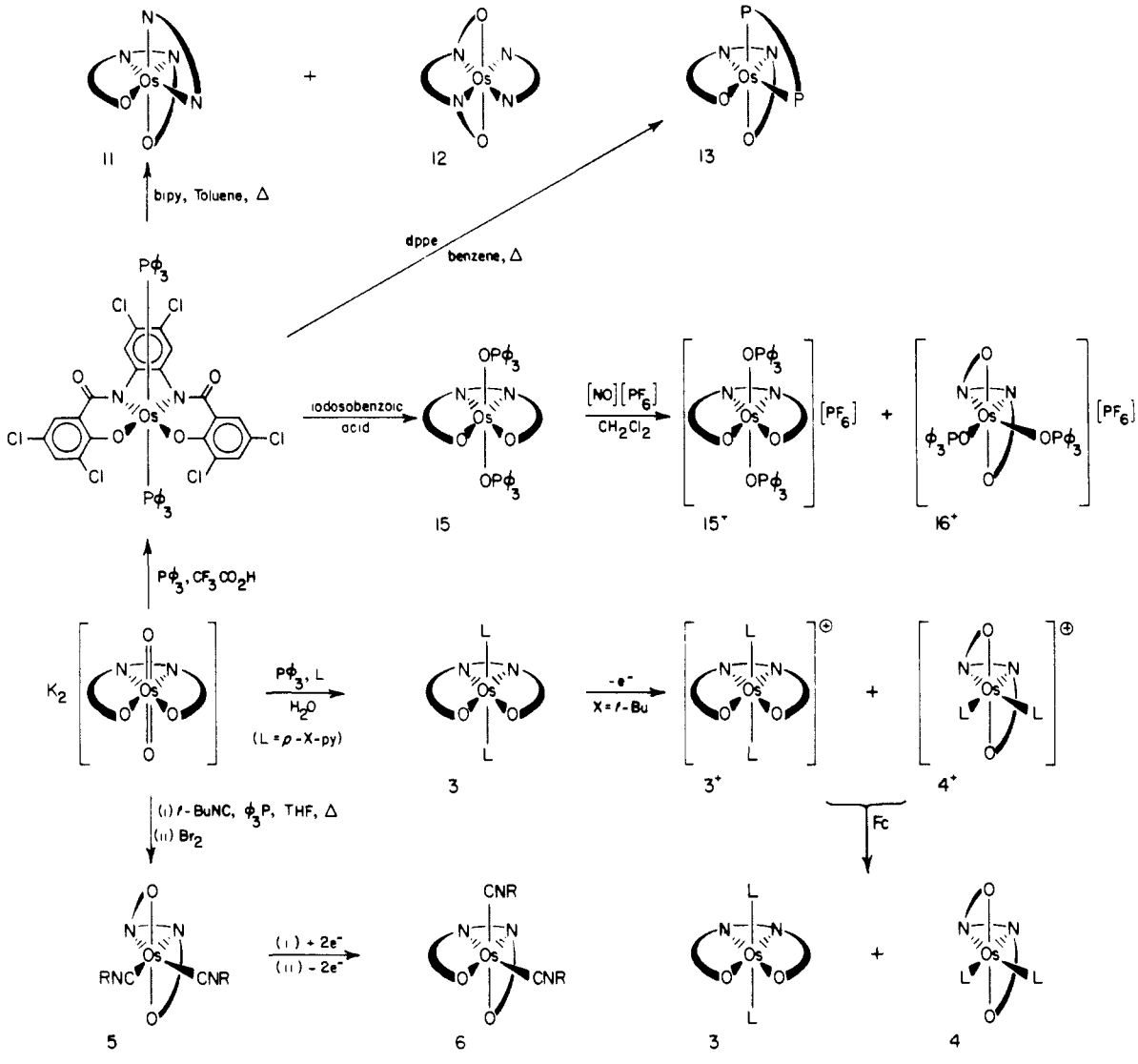

for the existence σ-backbonding in ruthenium and osmium systems are based upon a considerable quantity of experimental data.[24] Because the PAC ligand, $[\eta^4\text{-}1]^{4-}$, is such a powerful donor,[4,7,8,14] the third-row transition-metal complexes in the current study provide excellent systems for the examination of π-backbonding phenomena. In this light it is tempting to speculate that the increase in the deviation with increasing metal basicity signals the presence of unusual π-acceptor properties for *p*-acetylpyridine relative to the other pyridine ligands. The correlations are being extended to a wider family of substituted pyridines and to more basic PAC ligands to further explore the bonding parameters.

Nonplanar *N*-Amido Ligands. Evidence will now be presented to show that the monocation and osmium(IV) cis-α complexes contain nonplanar *N*-amido ligands. Recently we have structurally characterized several cis-α-osmium(IV) complexes of **1** (for synthetic routes to novel complexes of **1** see Scheme II) and **2** (see Scheme III) that contain distinctly nonplanar *N*-amido ligands (Scheme IV).[14] Coordination of a strong π-acid triggers isomerization to the cis-α diastereomer at the osmium(IV) stage. This contrasts with the bispyridine systems where a cis-α diastereomer is not observed until the monocation stage and further supports the theme that removal of electron density from the metal center favors the cis-α isomer. These structured complexes are distinguished by ν_{CO}(amide) IR bands that are shifted to higher frequencies (35–90 cm^{-1}) relative to the trans complexes that contain structurally normal planar amido ligands (ν_{CO}(amide) 1600–1620 cm^{-1}).[4-9] The shift is presumably due to the loss of amide resonance expected for the nonplanar form. The ν_{CO}(amide) bands are found at 1620 cm^{-1} for **3**, 1622 cm^{-1} for **3**$^+$, 1645 cm^{-1} for

Scheme III

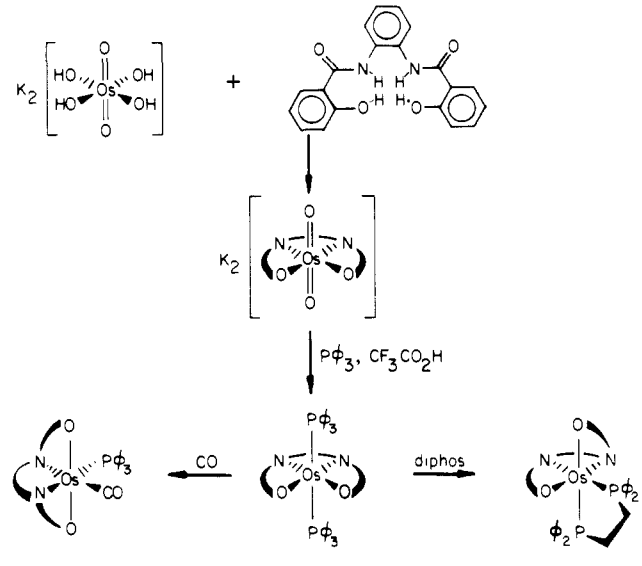

(24) (a) Creutz, C. *Prog. Inorg. Chem.* **1983**, *30*, 1–73. (b) Bino, A.; Lay, P. A.; Taube, H.; Wishart, J. F. *J. Am. Chem. Soc.* **1985**, *24*, 3969–3971, and references therein.

Scheme IV

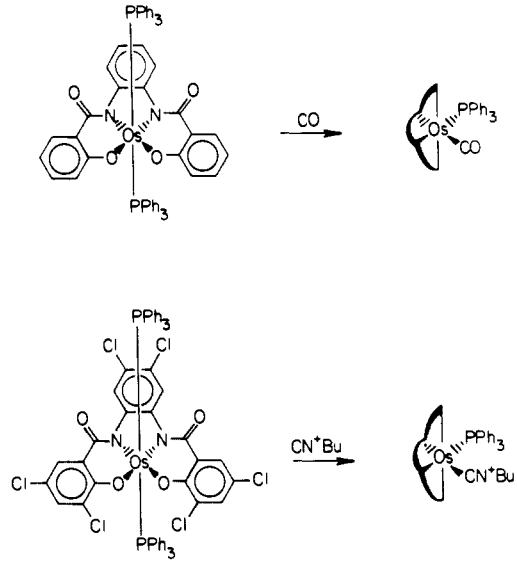

Table VI. IR Data for Complexes Containing Nonplanar *N*-amido Ligands [Planar Analogues Included] (cm^{-1})[g]

compound	ν_{CO} (nonplanar)	ν_{CO} (planar)
cis-α-[Os(η^4-**1**)($OPPh_3$)$_2$][PF_6], **16**$^+$	1681	
trans-[Os(η^4-**1**)($OPPh_3$)$_2$][PF]$_6$], **15**$^+$		1606
cis-α-Os(η^4-**1**)($OPPh_3$)$_2$, **16**	1626	
trans-Os(η^4-**1**)($OPPh_3$)$_2$, **15**		1608
cis-α-[Os(η^4-**1**)(*t*-Bupy)$_2$][ClO_4], **4**$^+$[e]	1679 br	
trans-[Os(η^4-**1**)(*t*-Bupy)$_2$][ClO_4], **3**$^+$[e]		1622
cis-α-Os(η^4-**1**)(*t*-Bupy)$_2$, **4**	1645 br	
trans-Os(η^4-**1**)(*t*-Bupy)$_2$, **3**		1620
cis-α-Os(η^4-**2**)(*t*-BuNC)(PPh_3)[a]	1680,[b] 1620[c]	
cis-α-Os(η^4-**2**)(CO)(PPh_3)[a]	1695,[d] 1637[c]	
cis-β-Os(η^4-**1**)(*t*-BuNC)$_2$, **5**	1694	1622
cis-α-Os(η^4-**1**)(*t*-BuNC)$_2$, **6**	1650	
cis-α-Os(η^4-**1**)(*t*-BuNC)(PPh_3)	1650 br	
cis-β-Os(η^4-**1**)(bipy), **11**[f]	1635	1622
cis-α-Os(η^4-**1**)(bipy), **12**[f]	1631	
cis-β-Os(η^4-**1**)(dppe), **13**	1670	1608
cis-β-Os(η^4-**2**)(dppe), **14**	1660	1590

[a] Assignment of the higher wavenumber ν_{CO} band to the amido ligand trans to the π-acid is based on structural information which shows greater distortion from planarity relative to the amido ligand trans to phosphine.[14] [b] Trans to isocyanide. [c] Trans to phosphine. [d] Trans to CO. [e] Measured in dichloromethane. [f] Measured in KBr pellet. [g] Measured as Nujol mulls unless otherwise stated.

4, and 1679 cm^{-1} for **4**$^+$. The increase found for the cis-α complexes is consistent with the presence of nonplanar amido ligands, with greater distortions from planarity being found for **4**$^+$ than for **4**. Higher amide ν_{CO} stretching frequencies are observed in nonplanar organic amides. For instance, spirodilactams have ν_{CO} values of 1641–1713 cm^{-1} depending on the degree of strain.[10s]

The work with π-acid ligands was extended by the synthesis of several additional osmium(IV) complexes, *cis*-α-Os(η^4-**1**)(*t*-BuNC)$_2$, **5**, and *cis*-α-Os(η^4-**2**)(*t*-BuNC)(PPh_3), where the cis-α diastereomers were again found to be thermodynamically stable at the osmium(IV) state. The ν_{CO}(amide) IR data suggests that all isolated cis-α (and cis-β vide infra) complexes contain *N*-amido ligands that are nonplanar to some degree (Table VI).

Since the cis-α diastereomer is stable only for oxidized metal centers, reduction of a π-acid containing *cis*-α-osmium(IV) complex should trigger isomerization to a trans or cis-β diastereomer; this does indeed occur. The purple complex, *cis*-α-Os(η^4-**1**)(*t*-BuNC)$_2$, **5**, is easily synthesized (Scheme II). IR and NMR evidence supports the cis-α formulation. Two infrared active bands in the isocyanide C–N stretching region found in both the solid state and solution spectra (2154 and 2002 cm^{-1}, Nujol mull) indicate that the complex is cis. The presence of one elevated

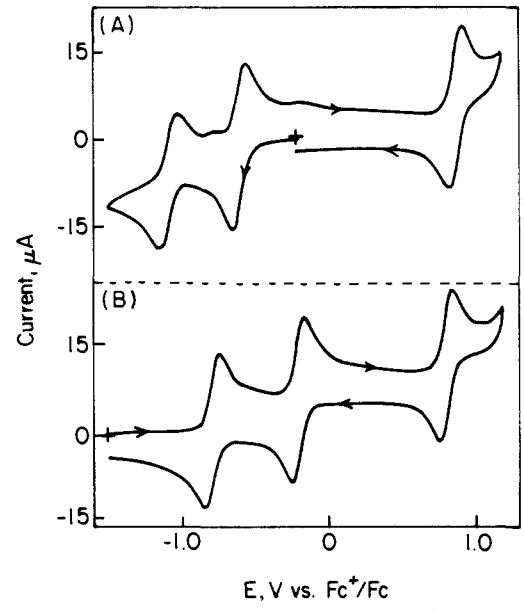

Figure 5. Cyclic voltammograms of 1.2 mM Os(η^4-**1**)(*t*-BuNC)$_2$ in CH_2Cl_2, 0.1 M TBAP at 0.03 cm^2 Pt electrode. Scan rate = 200 $mV \cdot s^{-1}$: (A) osmium(IV) and (B) osmium(II).

ν_{CO}(amide) band at 1650 cm^{-1} and the symmetry evident in the ^1H NMR spectrum support the cis-α formulation. The CV of a pure solution of **5** in dichloromethane is shown in Figure 5a. No change is observed upon reduction to osmium(III), but a new species is produced upon reduction to osmium(II) (Figure 5b). The new couples in Figure 5b are found at the same potentials as small waves that appear in the CV of the cis-α compound on cycling to osmium(II). Thus, the process that occurs upon formation of osmium(II) is rapid on the CV time scale. The CV of Figure 5b is retained upon reoxidation of the osmium(II) solution to osmium(IV). The new green osmium(IV) compound, **6**, was isolated and shown by ^1H NMR and IR to be the cis-β isomer of **5**. Upon heating under reflux in xylene, *cis*-β-**6** is converted completely to *cis*-α-**5**, with some decomposition. It is interesting to note that reduction to osmium(II) produces the cis-β and not the presumably less-donating trans ligand complement. The π-acid isocyanide ligands might be sufficiently electron-withdrawing to require that a more donating form than the trans complement be adopted. Alternatively, the mutually trans disposition of the π-acid isocyanide ligands in the trans diastereomer might be unfavorable. We favor the former explanation because controlled-potential electroreduction of *cis*-α-Os(η^4-**1**)(PPh_3)(*t*-BuNC) by 2 Faradays per mol also produces the cis-β isomer.

Evidence for Strong Donor Capacity of Nonplanar *N*-Amido Ligands. The reduction in amide resonance that accompanies distortions from planarity should increase the σ- and π-basicity of the amide nitrogen. We now present evidence which suggests that the nonplanar *N*-amido ligands play an important role both in the reduction of formal potentials found for the cis-α complexes and in the related increased donor capacities of the cis-α ligand complements. The complexes **7** and **8** were synthesized in a related study.[25a]

Consider the process of moving the in-plane phenolate donor of **3** to the axial position of **4**. In structurally characterized osmium(IV) complexes (Scheme IV) this movement is accommodated principally by rotation about the amide C–N bonds.[14] However, removal of the dichlorophenylene unit of **3**, as in **7**, should allow this movement to be accomplished by rotation about the Os–N bond, a process that would preserve amide planarity in **8**. The ν_{CO}(amide) IR bands are found at 1618 cm^{-1} for **7** and 1620 cm^{-1} for **8**, suggesting that planarity is indeed preserved in **8**. Thus, all the primary coordination sphere changes that occur

(25) (a) Krafft, T. E. Ph.D. Thesis, The California Institute of Technology, 1985. **7** was characterized by an X-ray crystal structure determination. (b) Gipson, S. L. Ph.D. Thesis, The California Institute of Technology, 1985.

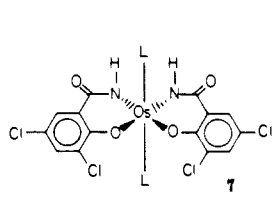
7

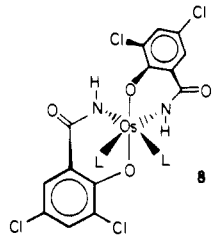
8

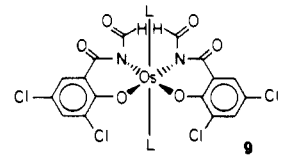
9

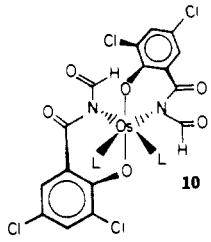
10

when **3** isomerizes to **4** are reproduced when **7** is converted to **8**, with the apparent exception that amide planarity is retained. In contrast to the formal potential differences for **3** and **4**, **7** and **8** exhibit very similar osmium(IV/III) and (III/II) formal potentials[25b] (−0.70, −1.99 for **7** and −0.70, −1.97, for **8**).[26,27] The monocation/osmium(IV) couples for **7** and **8** are irreversible. Unfortunately, at elevated temperatures complexes **7** and **8** show no tendency to isomerize before decomposition occurs making a determination of the equilibrium distribution for these two diastereomers impossible. However, the electrochemical data show that whatever the equilibrium constant for the **8** ⇌ **7** process is, it is little affected by reduction to lower oxidation states. Thus, if K^0, the equilibrium constant at the osmium(IV) oxidation state, is arbitrarily assigned a value of 1.00, then K^- also has a value of 1.00, K^{2-} has a value of 0.46. The structurally characterized compounds **9** and **10**[4a] also exhibit very similar osmium(IV/III) and (III/II) formal potentials (−0.39 and −1.88 V for **9**, −0.46 and −1.88 V for **10**, respectively).[28] These results suggest that the nonplanar N-amido ligands do play a significant role in the reduction in formal potentials observed for the *cis*-α-**4** series relative to the *trans*-**3** series of complexes and in the related increased donor capacities of the cis-α complements.

At this point *cis*-osmium(III) and *cis*-osmium(II) complexes have not been isolated. Thus, while reduced formal potentials are found for the *cis*-α- relative to the *trans*-osmium(III/II) couples, it should be noted that there is as yet no physical evidence for the presence of nonplanar amides in the cis complexes of these oxidation states.

Cis-β Complexes. It is interesting to note that a cis-β complex is not observed in cis-α ⇌ trans equilibria of the bispyridine complexes. In addition to **6**, several other cis-β complexes were produced in the course of this work. IR and X-ray structural evidence reveal that these complexes can also contain nonplanar *N*-amido ligands. The structurally characterized[4] *cis*-β-Os(η^4-**1**)(bipy), **11**, is an example of a complex containing both nonplanar and planar *N*-amido ligands.[30] Similarly, IR evidence suggests that *cis*-β-Os(η^4-**1**)(dppe), **13**, and *cis*-β-Os(η^4-**2**)(dppe), **14**, contain both nonplanar and planar N-amido ligands (Table VI). Complex **11** and the diastereomer *cis*-α-Os(η^4-**1**)(bipy), **12**, are produced as a mixture when *trans*-Os(η^4-**1**)$(PPh_3)_2$ is heated with 2,2′-bipyridine under reflux in toluene. The equilibrium constant could not be accurately determined because the forcing conditions required to effect the isomerization **11** ⇌ **12** also induced a significant amount of decomposition. The formal potentials for the osmium(IV/III) and -(III/II) couples for **11** (−0.49, −1.37 V) are more positive than those for **12** (−0.86, −1.45 V). However, the formal potentials for reduction of the monocations are similar (0.50 V for **11** and 0.49 V for **12**).

Oxidation of *trans*-Os(η^4-**1**)$(PPh_3)_2$ with iodosobenzoic acid affords *trans*-Os(η^4-**1**)$(OPPh_3)_2$, **15**, which, upon oxidation by 1 Faraday per mol, gives an equilibrium mixture of the trans and cis-α diastereomers, $\mathbf{15}^+$ and $\mathbf{16}^+$. Our mechanistic studies of the isomerization reactions of these phosphine oxide complexes at the osmium(IV) and monocation stages will be described in a subsequent publication.

Conclusion

It has been shown that the *trans*-$[Os(\eta^4\text{-}\mathbf{1})(p\text{-X-py})_2]^n$ complexes become increasingly favored upon stepwise reduction from the monocation to the dianion states. The cis-α ligand complement is the thermodynamically stable diastereomer at the neutral osmium(IV) stage when electron-withdrawing π-acid ligands are present. These results suggest that the complexes undergo the trans to cis-α structural change when increased donation is required by the metal center. It has been demonstrated that the cis-α complexes contain nonplanar *N*-amido ligands for the monocationic and osmium(IV) complexes, whereas the trans complexes contain planar *N*-amido ligands in these states. Because all the bonds in the cis-α and trans complexes are different (different trans ligands, etc.), one might have expected the significantly different donor capacities of the two ligand complements to be the sum of many small changes in σ-donor, π-donor, and π-acceptor properties for all the coordinated groups. However, the reduction in formal potentials observed for the cis-α complexes appears to be almost entirely dependent upon the presence of the nonplanar *N*-amido ligands. Thus, the overall increased donor capacities of the cis-α complements are also derived from this source. The equilibrium processes probably reflect a balance between the influence of amide resonance, which stabilizes the

(26) Measured in CH_2Cl_2/0.1 M TBAP and referenced to Fc^+/FC internal standard. Potentials in parentheses are the anodic peak potentials of irreversible oxidations.

(27) Both **7** and **8** are paramagnetic. This contrasts with all the systems containing tetradentate ligands reported in this work where the *cis*-α-osmium(IV) complexes are always diamagnetic, but the trans and cis-β diastereomers exhibit temperature independent paramagnetism. Changes in spin states should influence formal potentials, but the roles of spin state changes in the formal potential differences for the different diastereomers are unclear. Note that the diamagnetic cis-α complexes are more easily oxidized than their paramagnetic trans analogues, and not vice versa (see Table IV).

(28) Oxidation to the monocation could not be observed in dichloromethane or acetonitrile since oxidation of the medium occurred before any activity associated with these complexes could be detected.

(29) See footnote g Table III. $\Delta G^{\ddagger}$ was determined by variable temperature coalescence experiment as described in Sandstrom, J. *Dynamic NMR Spectroscopy*; Academic Press: New York, 1982; p 79. Coalescence of the H_m peaks occurred at 0 °C at 400 MHz. The frozen spectrum was recorded at −50 °C; $\delta\nu(H_m)$ = 174 Hz.

(30) Nonplanarity in organic amide groups is quantified according to the method of Dunitz et al. (a) Dunitz, J. D.; Winkler, F. K. *J. Mol. Biol.* **1971**, *59*, 169–182. (b) Dunitz, J. D.; Winkler, F. K. *Acta. Crystallogr., Sect. B: Struct. Crystallogr. Cryst. Chem.* **1975**, *B31*, 251–263. Definitions of amide nonplanarity parameters: $\tau = (\omega_1 + \omega_2)/2$, $|\omega_1 - \omega_2| < \pi$; $\chi_N = (\omega_2 - \omega_3 + \pi) \bmod 2\pi$; $\chi_C = (\omega_1 - \omega_3 + \pi) \bmod 2\pi$. Amide torsion angles are ω_1 = C–C–N–C; ω_2 = O–C–N–Os; ω_3 = O–C–N–C. The out-of-plane bending at the amide carbon, described by χ_C, is typically small. The out-of-plane bending at the amide nitrogen is described by χ_N. The parameters are represented in the accompanying projection down the amide C–N bond. For *cis*-β-Os(η^4-**1**)(bipy) where amide a = planar amide and amide b = nonplanar amide: ω_{1a} = 180 (2), ω_{2a} = −178 (2), ω_{3a} = −3 (3); ω_{1b} = 136 (2), ω_{2b} = 155 (2), ω_{3b} = −40 (3); χ_{Ca} = 3 (3), χ_{Na} = 5 (2), τ_a = 1 (3); χ_{Cb} = −4 (3), χ_{Nb} = 15 (2), τ_b = 145 (3). The angular parameters are represented in the accompanying diagram and detailed discussion of these parameters for all metallo-*N*-amido and related ligands can be found in ref 14. Notice that the nonplanar amide has a C–N bond rotation of 35° (180-τ_b) and is slightly pyramidalized at the nitrogen atom (χ_{Nb}). The root cause of the nonplanarity in this complex is related to the primary cause of nonplanarity in organic amides, viz. ring-strain factors.

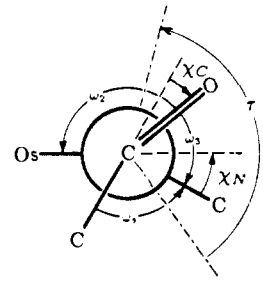

trans isomer, and increased donation from the nonplanar *N*-amido ligands in the cis-α ligand complements, which stabilizes the cis-α isomer in the more oxidized complexes. The increased donation probably also destabilizes the cis-α isomer in the more reduced species. The increase in ligand–metal bonding in the stable cis-α complexes is probably substantial, since rotational processes around the C–N bond of organic amides are typically subject to large activation barriers (10–35 kcal·mol^{-1}).[31] Note that these results imply that the trans to cis-α isomerizations occur so that nonplanar amido ligands can be produced rather than in spite of the production of nonplanar amido ligands.

An unexpected ligand design principle is implicit in this work. If *N*-amido PAC ligands are being designed to produce highly oxidizing metal complexes, then it might be important to design the PAC ligands such that spontaneous formation of nonplanar *N*-amido ligands cannot occur. Incorporation of the *N*-amido ligand in a relatively inflexible macrocyclic ligand might be a sufficient constraint.

Acknowledgment. We acknowledge the Rohm and Haas Co., the Atlantic Richfield Corporation of America, and the National Science Foundation (Grants CHE-84-06198 to T.J.C. and CHE-83-11579 to F.C.A.) for support of this work. S.L.G. thanks the NSF for the award of a predoctoral fellowship and the IBM Corporation for the award of an IBM fellowship. J.T.K. thanks SOHIO for the award of the SOHIO Fellowship in Catalysis, W.R. Grace for the award of the W.R. Grace Fellowship, and Shell for the award of the Shell Doctoral Fellowship. T.E.K. thanks the Union Carbide Corporation for the award of a Union Carbide Fellowship in Chemical Catalysis. We thank the Engelhard Corporation for a generous donation of precious metal compounds. We are especially grateful to Doug Meinhart for advice and instruction in NMR spectroscopic techniques. We thank Dr. Peter J. Desrosiers for recording the ^{31}P NMR spectrum of *cis*-β-Os(η^4-CHBA-DCB)(dppe). Operation of the Bruker WM-500 NMR spectrometer at the Southern California Regional NMR Facility was supported by the National Science Foundation Grant CHE-7916324. Operation of the SQUID susceptometer at the University of Southern California was supported in part by NSF Grant CHE-8211349.

(31) Stewart, W. E.; Siddall, T. H., III *Chem. Rev.* **1970**, *70*, 517–551.

Registry No. **3**-Cl, 103851-23-6; **3**-Cl$^+$, 103957-31-9; **3**-Cl$^-$, 103851-49-6; **3**-Cl^{2-}, 103957-47-7; **3**-Br, 104033-84-3; **3**-Br$^+$, 103851-38-3; **3**-Br$^-$, 103958-01-6; **3**-Br^{2-}, 103883-56-3; **3**-Me, 103851-24-7; **3**-Me$^+$, 103957-32-0; **3**-Me$^-$, 103957-44-4; **3**-Me^{2-}, 103957-49-9; **3**-Et, 103851-25-8; **3**-Et$^+$, 103957-33-1; **3**-Et$^-$, 103958-02-7; **3**-Et^{2-}, 103957-50-2; **3**-MeO, 103851-26-9; **3**-MeO$^+$, 103957-36-4; **3**-MeO$^-$, 103957-46-6; **3**-*t*-Bu, 90791-59-6; **3**-*t*-Bu$^+$ ClO_4^-, 103957-35-3; **3**-*t*-Bu$^-$, 103957-45-5; **3**-*t*-Bu^{2-}, 103957-51-3; **3**-Ac, 103851-27-0; **3**-Ac$^+$, 103957-30-8; **3**-Ac$^-$, 103851-48-5; **3**-Ac^{2-}, 103851-55-4; **3**-H$^+$, 103851-39-4; **3**-H$^-$, 103957-43-3; **3**-H^{2-}, 103957-48-8; **4**-*t*-Bu, 103957-26-2; **4**-*t*-Bu$^+$$ClO_4^-$, 103851-36-1; **4**-*t*-Bu$^-$, 103851-46-3; **4**-*t*-Bu^{2-}, 103851-54-3; **4**-Ac, 103957-37-5; **4**-Ac$^+$, 103851-30-5; **4**-Ac$^-$, 104011-49-6; **4**-Ac^{2-}, 103958-03-8; **4**-Cl, 103957-38-6; **4**-Cl$^+$, 103851-31-6; **4**-Cl$^-$, 103851-41-8; **4**-Cl^{2-}, 103851-50-9; **4**-Br, 103851-40-7; **4**-Br$^+$, 103851-32-7; **4**-Br$^-$, 103851-42-9; **4**-H, 103957-39-7; **4**-H$^+$, 103851-33-8; **4**-H$^-$, 103851-43-0; **4**-H^{2-}, 103851-51-0; **4**-Me, 103957-40-0; **4**-Me$^+$, 103851-34-9; **4**-Me$^-$, 103851-44-1; **4**-Me^{2-}, 103851-52-1; **4**-Et, 103957-41-1; **4**-Et$^+$, 103851-35-0; **4**-Et$^-$, 103851-45-2; **4**-Et^{2-}, 103851-53-2; **4**-MeO, 103957-42-2; **4**-MeO$^+$, 103851-37-2; **4**-MeO$^-$, 103851-47-4; **5**, 103957-27-3; **6**, 103957-28-4; **11**, 90791-61-0; **12**, 103957-29-5; **13**, 103883-55-2; **14**, 103851-28-1; **15**, 103851-29-2; **15**$^+$, 103851-59-8; **16**, 103958-00-5; **16**$^+$, 103957-53-5; H_4CHBA-DCB, 90791-63-2; H_4HBA-B, 103528-00-3; K_2[*trans*-Os(η^4-**2**)$(O)_2$], 103851-56-5; *trans*-Os(η^4-**2**)$(PPh_3)_2$, 90791-57-4; K_2[*trans*-Os(η^4-**2**)$(O)_2$], 103851-57-6; K_2[Os$(OH)_4(O)_2$], 77347-87-6; *cis*-α-Os(η^4-**2**)(*t*-BuNC)(PPh_3), 103883-57-4; K_2[*trans*-Os(η^4-**1**)$(O)_2$], 90791-56-3; *trans*-Os(**1**)$(PPh_3)_2$, 90791-57-4; *cis*-α-Os(η^4-**1**)(*t*-BuNC)(PPh_3), 103191-19-1; *cis*-α-Os(η^4-**1**)(*t*-BuNC)(PPh_3), 103191-20-4; PPh_3, 603-35-0; 2-acetylsalicylic acid, 50-78-2; *o*-phenylenediamine, 95-54-5.

A New Magic Cluster Electron Count and Metal–Metal Multiple Bonding

Ralph A. Wheeler and Roald Hoffmann*

Contribution from the Department of Chemistry and Materials Science Center, Cornell University, Ithaca, New York 14853-1301. *Received May 5, 1986*

Abstract: Metal–metal multiple bonding radically alters the preferred electron count for trigonal-prismatic clusters. The recently synthesized $Tc_6Cl_{12}^{2-}$ and $Tc_6Cl_{14}^{3-}$ have short Tc–Tc bonds parallel to the prism's threefold axis. $Tc_6Cl_{12}^{2-}$ has 32 metal electrons and $Tc_6Cl_{14}^{3-}$ has 31. A molecular orbital analysis of the bonding in $Tc_6Cl_{12}^{2-}$ shows essentially electron rich ($\sigma^2\pi^4\delta^2\delta^{*2}$) triple bonding within each dimer unit, single bonds in the triangles, and two electrons in an a_2'' orbital that is π^* with respect to the dimers, weakly bonding in the triangles. The a_2'' is net antibonding, so that the number of framework bonding electrons in this structure is only 30. This is a very different magic number from the 16, 24, or 14 known for octahedra and 18 for trigonal prisms. One-electron oxidation affects $Tc_6Cl_{14}^{3-}$ bonding in a predictable way; we also discuss the Tc_8Br_{12} structure.

Kryuchkov, Kuzina, and Spitsyn recently synthesized two Tc clusters, $Tc_6Cl_{12}^{2-}$ and $Tc_6Cl_{14}^{3-}$ (**1** and **2**),[1a-d] which stand at the intersection of two important directions of modern inorganic chemistry—namely, cluster chemistry and metal–metal multiple bonding.

(1) (a) Kryuchkov, S. V.; Kuzina, A. F.; Spitsyn, V. I. *Dokl. Akad. Nauk SSSR* **1982**, *266*, 127; *Dokl. Akad. Nauk SSSR (Engl. Transl.)* **1982**, *266*, 304. (b) German, K. E.; Kryuchkov, S. V.; Kuzina, A. F.; Spitsyn, V. I. *Dokl. Akad. Nauk SSSR* **1986**, *288*, 381. (c) Spitsyn, V. I.; Kuzina, A. F.; Oblova, A. A.; Kryuchkov, S. V. *Uspek. Khim.* **1985**, *54*, 637; *Russ. Chem. Rev.* **1985**, *54*, 373. (d) For a related octahedral cluster see: Kryuchkov, S. V.; Kuzina, A. F.; Spitsyn, V. I. *Dokl. Akad. Nauk SSSR* **1986**, *287*, 1400. (e) Koz'min, P. A.; Surazhskaya, M. D.; Larina, T. B. *Koord. Khim.* **1985**, *11*, 1559. (f) Koz'min, P. A.; Surazhskaya, M. D.; Larina, T. B. *Dokl. Akad. Nauk SSSR* **1983**, *271*, 1157.

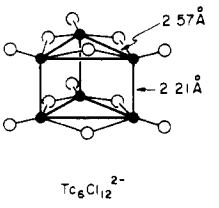

1

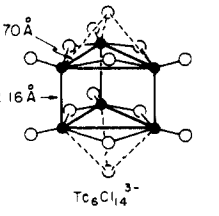

2

Let us first describe these compounds, whose structures were determined by Koz'min, Surazhskaya, and Larina,[1e,f] and then pinpoint their significance. **1** and **2** are both trigonal prisms of metal atoms. In each, every technetium has one terminal chloride;

0002-7863/86/1508-6605$01.50/0